STARK BROADENING IN LASER-PRODUCED PLASMAS:
FULL COULOMB CALCULATION

BY

LAWRENCE A. WOLTZ

A DISSERTATION PRESENTED TO THE GRADUATE COUNCIL
OF THE UNIVERSITY OF FLORIDA IN
PARTIAL FULFILLMENT OF THE REQUIREMENTS
FOR THE DEGREE OF DOCTOR OF PHILOSOPHY

UNIVERSITY OF FLORIDA

AUGUST 1982

TABLE OF CONTENTS

STARK BROADENING IN LASER-PRODUCED PLASMAS:
FULL COULOMB CALCULATION

by

Lawrence A. Woltz

August, 1982

This work is a study of the Stark broadening of spectral lines
emitted by highly charged ions in a hot, dense plasma. The line
broadening calculations of Tighe and Hooper, in which the dipole
approximation was used for the interaction between the radiating ions
and perturbing electrons, are extended by retaining the full Coulomb
radiator-perturbing electron interaction. Electron broadening is
treated to second order in the radiator-perturbing electron interaction;
ion broadening is treated by a static ion microfield probability
distribution. Perturbing electrons are treated quantum mechanically
through Coulomb wavefunctions to account for the charged radiator.

Line profiles from this calculation are slightly broader than those
calculated using the dipole approximation. The near agreement of these
results is partly fortuitous in that the dipole approximation
overestimates the dipole part of the Coulomb interaction for perturbers
close to the radiator, partially compensating for the neglected

iv

multipoles of the interaction. This full Coulomb calculation of the dynamic line shift due to perturbing electrons results in a significantly smaller shift than that obtained when the dipole approximation for the radiator-perturbing electron interaction is used. For an Argon Lyman β line calculated for the plasma conditions of 10^{24} electrons/cm^3 and 800 eV, this shift is about 0.03 Ryd toward lower energies, and it causes no noticeable asymmetry in the line. The effect of the dynamic shift on the line is considerably smaller than that of the static (plasma polarization) shift calculated by Skupsky, which causes an asymmetry in the β line, with the red wing having the greater intensity. For an Argon Lyman β line, the significance of ion-radiator and electron-radiator perturbation matrix elements between the initial radiator states, principal quantum number = 3, and the states of the nearest adjacent energy level, principal quantum number = 4, is examined. The electron-radiator matrix elements are found to give a small additional broadening of the line; the ion-radiator matrix elements are found to cause a significant nonlinear Stark shift of the radiator energy levels. This shift causes the line to be asymmetric, with the blue peak having greater intensity than the red peak and the red wing having greater intensity than the blue wing.

CHAPTER I
PLASMA SPECTRAL LINE BROADENING

I.1 Introduction

Plasma broadened spectral lines have been used for many years in
determining the densities and temperatures of laboratory and astro-
physical plasmas (Griem 1964, 1974; Baranger 1962; Cooper 1966; Smith,
Cooper, and Vidal 1969, 1970). Recently, plasma broadened X-ray spectra
from highly ionized high-Z elements (e.g. neon or argon) have been used
to determine the densities of laser inertial confinement plasmas
(Yaakobi et al. 1977, 1979, 1980; Kilkenny et al. 1980; Apruzese et al.
1981).

The purpose of this work is to extend theoretical line shape calcu-
lations by Tighe (1977) and Tighe and Hooper (1976, 1978), which were
used in the studies of Yaakobi et al. The work of Tighe and Hooper is
an adaptation of the relaxation theory of line broadening (Smith 1966;
Smith and Hooper 1967; O'Brien 1970; O'Brien and Hooper 1974) to hydro-
genic radiators of arbitrary charge, appropriate for the high-Z
radiators of laser implosion experiments. In the Tighe-Hooper calcula-
tions the dipole approximation is made for the radiator-perturbing
electron interaction, an approximation which is of questionable validity
at the high densities obtained in some recent experiments. In this line
shape calculation we will not make the dipole approximation but will
retain the full Coulomb radiator-perturbing electron interaction.

1

In this chapter we outline a line broadening theory which is obtained by use of the kinetic theory of time correlation functions (Hussey 1974; Hussey et al. 1975), then apply several approximations to obtain a theory in which the line width and shift operator is expanded to second order in the radiator-perturbing electron potential. In Chapter II we develop a computational form for the full Coulomb second order theory. In Chapter III we present Lyman series line shapes calculated numerically from the formalism of Chapter II. We compare profiles calculated from this full Coulomb theory with the results of Tighe and Hooper, and also compare this calculation to a recent impact theory of line broadening (Griem et al. 1979). Calculated line shapes which include dynamic shift and inelastic effects are also presented.

I.2 The Line Shape

The power spectrum emitted by one type of ion in a plasma can be written in terms of the ensemble-averaged radiation emitted by one ion of that type (the radiator) as (Griem 1974)

$$P(\omega) = \frac{4\omega^4}{3c^3} \sum_{ab} |\langle a|\vec{d}|b\rangle|^2 \rho_a \delta(\omega - \omega_{ab}) \qquad (1.2.1)$$

where ρ_a is the probability that the radiator-plasma system is in the state $|a\rangle$, $\vec{d}$ is the dipole moment of the radiator, and $\omega_{ab} = (E_a - E_b)/\hbar$. The line shape function $I(\omega)$ is defined in terms of the power spectrum by the equation

$$P(\omega) = \frac{4\omega^4}{3c^3} I(\omega),$$

where

$$I(\omega) = \sum_{ab} |\langle a|\vec{d}|b\rangle|^2 \, \rho_a \delta(\omega-\omega_{ab}). \qquad (1.2.2)$$

We can express the Dirac delta function in $I(\omega)$ as an integral to obtain

$$I(\omega) = \frac{1}{2\pi} \int_{-\infty}^{\infty} \sum_{ab} |\langle a|\vec{d}|b\rangle|^2 \rho_a \, e^{i(\omega-\omega_{ab})t}dt. \qquad (1.2.3)$$

Here, the integrand for negative values of t is equal to the complex conjugate of the integrand for positive values of t, so we can rewrite this equation in terms of an integral from zero to infinity:

$$I(\omega) = \frac{1}{\pi} \, \mathrm{Re} \int_{0}^{\infty} \sum_{ab} |\langle a|\vec{d}|b\rangle|^2 \, \rho_a \, e^{i(\omega-\omega_{ab})t}dt \qquad (1.2.4)$$

or

$$I(\omega) = \frac{1}{\pi} \, \mathrm{Re} \int_{0}^{\infty} \sum_{ab} e^{i\omega t}\langle b|\vec{d}|a\rangle \cdot \langle a| \, \rho e^{-iHt/\hbar} \, \vec{d} e^{iHt/\hbar}|b\rangle dt \ , \qquad (1.2.5)$$

where H is the Hamiltonian for the radiator-plasma system and ρ is the canonical density operator, $\rho = e^{-\beta H}/\mathrm{Tr} \, e^{-\beta H}$. This can be written as

$$I(\omega) = \frac{1}{\pi} \, \mathrm{Re} \, \mathrm{Tr} \int_{0}^{\infty} dt \, e^{i\omega t} \, \vec{d} \cdot \rho \, e^{-iHt/\hbar} \, \vec{d} \, e^{iHt/\hbar}, \qquad (1.2.6)$$

where Tr represents a trace over states of the radiator-plasma system.

In Eq. (1.2.1) we have neglected Doppler broadening of the line shape due to the motion of the radiator. This will be included approximately at the end of the calculation by convoluting the line shape with a Doppler profile based on a Maxwell velocity distribution. This is an approximate treatment of Doppler broadening based on the

assumption that the change of momentum of the radiator is negligible during the time of radiation (Smith et al. 1971a, 1971b). The Doppler profile is given by

$$I_D(\omega) = \frac{1}{\gamma\sqrt{\pi}}\, e^{-(\omega-\omega_o)^2/\gamma^2} , \qquad (1.2.7)$$

where

$$\gamma^2 = \frac{2kT}{Mc^2}\,\omega_o^{\;2},$$

M is the mass of the radiator, and ω_o is the frequency of the unperturbed transition.

I.3 Time Scales

The line shape is given by the Laplace transform of the radiator dipole autocorrelation function (Eq. 1.2.6). Since the transform has the property $\Delta\omega\Delta t \lesssim 1$, where $\Delta\omega$ is the frequency separation from the line center, the time dependence of a perturbation of the radiator which changes significantly in time τ will be evidenced by the the part of the line for which $\Delta\omega \lesssim 1/\tau$. For $\Delta\omega \gg 1/\tau$, the perturber can be considered as static. This part of the line corresponds to radiation from initial radiator states having average lifetimes much shorter than τ. In the plasma line broadening problem there are two characteristic perturbation times, $\tau_i \sim 1/\omega_{pi}$ for perturbations due to ions and $\tau_e \sim 1/\omega_{pe}$ for perturbations due to electrons, where ω_{pe} and ω_{pi} are the electron and ion plasma frequencies.

For the plasma conditions which we will examine, the half-widths of the first few Lyman lines fall within the region $\Delta\omega < \omega_{pe}$, so we must treat the perturbation due to the electrons as a dynamic process. In

the case of the ions, the region $\Delta\omega < \omega_{pi}$ corresponds to only a small part of the line center. We will therefore ignore ion dynamic effects and make the approximation that the perturbing ions and radiator are static and that the ions perturb the radiator through a static electric field. This approximation, which is used in many line broadening calculations, is known as the Static Ion Approximation. Lyman line shapes which include ion motion effects have been calculated for hydrogen plasmas (Greene 1979; Seidel 1980). There, the inclusion of ion motion was found to cause additional broadening near the line center. The peak of the Lyman alpha line was significantly lowered, the peaks of the Lyman beta line were lowered slightly and the central dip was raised.

I.4 The Ion Microfield

In this section we apply two approximations which will permit us to write the line shape expression in the form

$$I(\omega) = \int_0^\infty P(\varepsilon)J(\omega,\varepsilon) \qquad (1.4.1)$$

where $P(\varepsilon)$ is the low frequency ion microfield probability (Baranger and Mozer 1959; Mozer and Baranger 1960; Hooper 1968; O'Brien and Hooper 1974; Tighe and Hooper 1977) and $J(\omega,\varepsilon)$ is the line shape due to the electron broadening of radiators in the presence of the ion microfield $\vec{\varepsilon}$. The Hamiltonian for the radiator and plasma is

$$H = H_r + H_i + H_e + V_{ri} + V_{re} + V_{ie} \qquad (1.4.2)$$

where H_r, H_i, and H_e are the Hamiltonians for the radiator, ion, and electron systems, V_{ri}, V_{re}, and V_{ie} are the potential energies between the radiator and ions, radiator and electrons, and ions and electrons. The effect of the interaction V_{ie} is to correlate the ions and electrons such that the average electron density is greatest near the ions. Therefore, the field at the radiator due to the electrons has a low frequency component which tends to partially cancel the ion field there. If the average electron spacing is much less than the Debye length, i.e.

$$n_e^{-1/3} \ll \lambda_D = (\frac{kT}{4\pi n_e e^2})^{1/2} , \qquad (1.4.3)$$

where n_e is the electron density, and quantum mechanical effects are not significant (Iglesias 1982), we can treat this correlation effect to a good approximation by considering the low frequency microfield at the radiator to be due to Debye screened ion fields (Baranger 1962). Similarly, we can consider the ion-ion interaction to be screened by the electrons. With the effects of V_{ie} approximated by screening, we eliminate it from the Hamiltonian to obtain

$$H = (K_i + V_i^S + \phi_{ri}) + (H_r + H_e + V_{re} + e \, \vec{\varepsilon}_i \cdot \vec{x}_r)$$

$$= H_i' + H' , \qquad \qquad (1.4.4)$$

where H_i' is the Hamiltonian for the ions and H' is the Hamiltonian for the radiator and electrons. Here, K_i is the ion kinetic energy, V_i^S is the shielded ion-ion potential energy, H_e is the Hamiltonian for an electron gas, ϕ_{ri} is the monopole part of the shielded ion-radiator

potential, $\vec{\varepsilon}_i$ is the shielded ion field,

$$\vec{\varepsilon}_i = \sum_j \frac{Z_j e \vec{x}_j}{x_j^3} \left(1 + \frac{x_j}{\lambda_D}\right) e^{-x_j/\lambda_D} , \qquad (1.4.5)$$

and $\vec{x}_r$ and $\vec{x}_j$ are the positions of the radiator electron and the j'th ion with respect to the radiator nucleus, which we choose as the origin of our coordinate system. We will neglect terms of higher order than dipole in the radiator-ion interaction. This approximation is much better for the ions than for the electrons in the case of high Z per-turbers since the ion density is $1/Z_{ion}$ times the electron density and since the large ion-radiator repulsion tends to keep the ions and radiator apart. However, for deuterium-tritium plasmas with a small amount of high-Z impurity, terms of higher order than dipole in V_{ri} may have a significant effect on the line shape.

We also use the static ion approximation. We assume that the ions do not move significantly during the lifetime of the initial radiator state, so we make the approximation

$$i\hbar \frac{\partial H_i'}{\partial t} = \left[H_i', H\right] = 0. \qquad (1.4.6)$$

Then the time evolution and density operators can be factored,

$$e^{iHt/\hbar} = e^{iH't/\hbar} e^{iH_i't/\hbar} , \qquad (1.4.7)$$

and

$$\rho = \rho_i \rho_{re} , \qquad (1.4.8)$$

where

$$\rho_i = e^{-\beta H_i'} / \text{Tr}_i \, e^{-\beta H_i'} \qquad (1.4.9)$$

and

$$\rho_{re} = e^{-\beta H'}/Tr_{re} \, e^{-\beta H'} \quad . \qquad (1.4.10)$$

The line shape then is given by

$$I(\omega) = \frac{1}{\pi} \, \text{Re} \, Tr_i \rho_i \int_0^\infty dt \, e^{i\omega t} \, \vec{d} \cdot Tr_{re} \, \rho_{re} \, e^{-iH't/\hbar} \, \vec{d} \, e^{iH't/\hbar} \quad .$$

$$(1.4.11)$$

Next we multiply this equation by $\delta(\vec{\varepsilon}-\vec{\varepsilon}_i)$ and integrate over $\vec{\varepsilon}$ to obtain

$$I(\omega) = \int \, Q(\vec{\varepsilon}) J(\omega,\vec{\varepsilon}) d\vec{\varepsilon} \quad ,$$

where

$$Q(\vec{\varepsilon}) = Tr_i \rho_i \, \delta(\vec{\varepsilon}-\vec{\varepsilon}_i) \qquad (1.4.12)$$

is the probability of finding the ion microfield $\vec{\varepsilon}$ at the radiator,

$$J(\omega,\varepsilon) = \frac{1}{\pi} \, \text{Re} \, Tr_{re} \int_0^\infty dt \, e^{i\omega t} \, \vec{d} \cdot \rho_{re} \, e^{-iH'(\vec{\varepsilon})t/\hbar} \, \vec{d} \, e^{iH'(\vec{\varepsilon})t/\hbar} \quad ,$$

and

$$H'(\vec{\varepsilon}) = H_r + H_e + V_{er} + e\vec{\varepsilon}\cdot\vec{x}_r \quad .$$

Since we consider an isotropic plasma, we can define the probability of finding the ion microfield of ·magnitude ε at the radiator by $P(\varepsilon) = 4\pi\varepsilon^2 Q(\vec{\varepsilon})$. Then

$$I(\omega) = \int_0^\infty \, P(\varepsilon) J(\omega,\varepsilon) d\varepsilon \qquad (1.4.13)$$

and

$$J(\omega,\varepsilon) = \frac{1}{\pi} \, \text{Re} \, Tr_{re} \int_0^\infty dt \, e^{i\omega t} \, \vec{d} \cdot \rho_{re} \, e^{-iH'(\varepsilon)t/\hbar} \, \vec{d} \, e^{iH'(\varepsilon)t/\hbar} \quad ,$$

$$(1.4.14)$$

where

$$H'(\varepsilon) = H_r + H_e + V_{er} + e\varepsilon z_r .$$

$$= H(r) + H_e + V_{er} .$$

For convenience, we have chosen the z-axis to be in the direction of the field $\vec{\varepsilon}$.

I.5 Kinetic Theory

Here we follow the work of Hussey (1974) and Hussey et al. (1975) to obtain an expression for $J(\omega,\varepsilon)$ in terms of a width and shift operator, $M(\omega)$. The advantage of this form is that results obtained by approximate treatments of $M(\omega)$ are much better than those obtained when similar approximations are applied directly to $J(\omega,\varepsilon)$.

We define the Liouville operator L in terms of a commutator of the Hamiltonian $H'(\varepsilon)$,

$$Lf = [H',f]/\hbar \qquad (1.5.1)$$

and write $J(\omega,\varepsilon)$ as

$$J(\omega,\varepsilon) = \frac{1}{\pi} \, \text{Re} \, \text{Tr}_{re} \int_0^\infty e^{i\omega t} \, \vec{d} \cdot \rho_{re} \, e^{-iLt} \, \vec{d} \ . \qquad (1.5.2)$$

We then define the radiator and s-perturber functions

$$n^s \, \vec{F}(r,1,\ldots,s;t) = \frac{N!}{(N-s)!} \, \text{Tr}_{s+1\ldots N} \, \rho_{re} \, e^{-iLt} \, \vec{d} \ , \qquad (1.5.3)$$

where $Tr_{s+1...N}$ is a trace over perturbing electrons $s+1$ through N and n is the electron density. We can then write $J(\omega,\varepsilon)$ in terms of the $s=0$ function $\vec{F}(r;t)$ or its Laplace transform $\vec{F}(r;\omega)$ as

$$J(\omega,\varepsilon) = \frac{1}{\pi} \text{ Re Tr}_r \int_0^\infty dt \ e^{i\omega t} \ \vec{d}\cdot\vec{F}(r;t)$$

$$= \frac{1}{\pi} \text{ Re Tr}_r \ \vec{d}\cdot\vec{F}(r;\omega) \ . \tag{1.5.4}$$

If we take a partial time derivative of Eq. (1.5.3) we obtain

$$[\frac{\partial}{\partial t} + iL(r,1,...,s;t)]\vec{F}(r,1,...,s;t) =$$

$$- \ in \ Tr_{s+1}[L_1(r,s+1) + \sum_{i=1}^{s} L_2(i,s+1)]\vec{F}(r,1,...,s+1;t) \ ,$$
$$\tag{1.5.5}$$

where

$$L(r,1,...,s;t)f = \left[H(r) + H_e(1,...,s) + V_{er}(1,...,s),f \right] \ ,$$

$$L_1(r,1)f = \left[V_1(r,1),f \right]/\hbar \ ,$$

$$L_2(1,2)f = \left[V_2(1,2),f \right]/\hbar \ ,$$

$V_1(r,1)$ is the interaction between the radiator and perturber 1, and $V_2(1,2)$ is the interaction between perturbers 1 and 2. Equation (1.5.5) relates the s-perturber function $\vec{F}(r,1,...,s;t)$ to the s+1-perturber function $\vec{F}(r,1,...,s+1;t)$, so we have an infinite hierarchy of equations, the BBGKY hierarchy (Bogoliubov 1962). We will formally close

the hierarchy to obtain an equation for $\vec{F}(r;\omega)$, and therefore $J(\omega,\varepsilon)$, in terms of a width and shift operator, $M(\omega)$, to be defined later.

We define the radiator and s-perturber reduced distribution functions,

$$n^s f(r,1,\ldots,s) = \frac{N!}{(N-s)!} \, Tr_{s+1\ldots N} \, \rho_{re} \, ,\qquad (1.5.6)$$

and the time evolution operator

$$U(r,1,\ldots,s;t) = \frac{N!}{n^s(N-s)!} \, Tr_{s+1\ldots N} \, \rho_{re} \, e^{-iLt} \, f(r,1,\ldots,s)^{-1}$$

$$(1.5.7)$$

such that

$$\vec{F}(r,1,\ldots,s;t) = U(r,1,\ldots,s;t)\vec{F}(r,1,\ldots,s;t=0)$$

$$= U(r,1,\ldots,s;t)f(r,1,\ldots,s)\vec{d}. \qquad (1.5.8)$$

The closure relation is obtained by eliminating $\vec{d}$ from the s=0 and arbitrary-s members of the Laplace transform of Eq. (1.5.8),

$$\vec{F}(r,1,\ldots,s;\omega) = U(r,1,\ldots,s;\omega)f(r,1,\ldots,s)f(r)^{-1}U(r;\omega)^{-1}\vec{F}(r;\omega) \, ,$$

$$(1.5.9)$$

where

$$U(r,1,\ldots s;\omega) = \frac{N!}{n^s(N-s)!} \, Tr_{s+1\ldots N} \, \rho_{re} i(\omega-L)^{-1} f(r,1,\ldots,s)^{-1} .$$

$$(1.5.10)$$

This equation for s=1 is substituted for $\vec{F}(r,1;\omega)$ in the Laplace transformed first equation of the hierarchy to obtain

$$\left[-i\omega + iL(r)\right]\vec{F}(r;\omega) - f(r)\vec{d} =$$

$$-inTr_1L_1(r,1)\left[U(r,1;\omega)f(r,1)f(r)^{-1}U(r;\omega)^{-1}\right]\vec{F}(r;\omega). \qquad (1.5.11)$$

Then we separate the term in brackets on the right side of Eq. (1.5.11) into frequency dependent and frequency independent parts by defining

$$U(r,1,\ldots,s;\omega)f(r,1,\ldots,s)f(r)^{-1}U(r;\omega)^{-1} =$$

$$K(r,1,\ldots,s;\omega) + f(r,1,\ldots,s)f(r)^{-1} \qquad (1.5.12)$$

and solve for $\vec{F}(r;\omega)$ to obtain

$$\vec{F}(r;\omega) = i\left[\omega - L(r) - B - M(\omega)\right]^{-1} f(r)\vec{d} , \qquad (1.5.13)$$

where

$$B = nTr_1L_1(r,1)f(r,1)f(r)^{-1} , \qquad (1.5.14)$$

$$M(\omega) = nTr_1L_1(r,1)K(r,1;\omega) . \qquad (1.5.15)$$

Similarly, we can use the second equation of the hierarchy (Eq. 1.5.5) to obtain for $K(r,1;\omega)$ (Hussey 1974; Hussey et al. 1975):

$$K(r,1;\omega) = \left[\omega - L(r,1) - V(r,1;\omega)\right]^{-1} f(r,1) \mathcal{L}(r,1) f(r)^{-1} \qquad (1.5.16)$$

where

$$V(r,1;\omega) = -nf(r,1)f(r)^{-1} \, Tr_2 L_1(r,2) P_{12}$$

$$+ nTr_2\left[L_1(r,2) + L_2(1,2)\right] G(r,1,2;\omega) G(r,1;\omega)^{-1}$$

and

$$\mathcal{L}(r,1) = L_1(r,1) + nf(r,1)^{-1} \, Tr_2\left[f(r,1,2)\right.$$

$$\left. - f(r,1)f(r)^{-1}f(r,2)\right] L_1(r,2) \; . \qquad (1.5.17)$$

The operator P_{12} acts to the right to change the argument 1 to 2. We use Eq. (1.5.16) in Eq. (1.5.15) to obtain

$$M(\omega) = nTr_1 L_1(r,1)\left[\omega - L(r,1) - V(r,1;\omega)\right] f(r,1) \mathcal{L}(r,1) f(r)^{-1} \; .$$
$$(1.5.18)$$

With Eqs. (1.5.4) and (1.5.13) we can now write $J(\omega,\varepsilon)$ as

$$J(\omega,\varepsilon) = -\frac{1}{\pi} \, Im \, Tr_r \cdot \vec{d} \cdot \left[\omega - L(r) - B - M(\omega)\right]^{-1} f(r) \vec{d} \; . \qquad (1.5.19)$$

Here, the effects of the plasma electrons on the line shape are contained in B and $M(\omega)$. The operator B is a mean field or Hartree-Fock type term which represents the shift of radiator energy levels due to polarization of the plasma by the radiator. The real and imaginary

parts of the operator $M(\omega)$ represent the dynamic shift and width, respectively, due to finite time collisional effects. The operator $\mathscr{L}(r,1)$ is the interaction of the radiator and perturber 1 statically screened by the other perturbing electrons.

I.6 Second Order Theory

In this section we restrict the width and shift operator, $M(\omega)$, to second order in the radiator-perturbing electron interaction, $V_1(r,1)$. We also make use of other approximations which are common to many line shape calculations: the neglect of interactions between perturbing electrons (The correlation effects thus neglected will be reintroduced in an approximate manner later in the calculation), the No-Quenching Approximation (NQA), and the No Lower State Broadening Approximation (NLBA).

The neglect of perturbing electron interactions permits us to write the electron Hamiltonian as a sum of single-particle Hamiltonians,

$$H_e = \sum_i H(i) \; . \tag{1.6.1}$$

Since the radiator is at the origin of our coordinate system, the long range monopole part of the radiator-perturber interaction, $-(Z-1)e^2/x_1$, is a function of only the perturber coordinate $\vec{x}_1$. Therefore we include it in the one-electron Hamiltonian, $H(1)$, by redefining $H(1)$ and $V_1(r,1)$ as

$$H(1) = \frac{p_1^2}{2m} - \frac{(Z-1)e^2}{x_1} \tag{1.6.2}$$

and

$$V_1(r,1) = \frac{e^2}{|\vec{x}_r - \vec{x}_1|} - \frac{e^2}{x_1} \; . \tag{1.6.3}$$

We can now expand $M(\omega)$ in this short ranged $V_1(r,1)$ while retaining to all orders the effect of the radiator monopole on the perturbing electrons.

For the plasma conditions and Lyman lines which we will consider, a large part of each line satisfies $\Delta\omega \lesssim \omega_{pe}$, where $\Delta\omega$ is the frequency separation from line center and ω_{pe} is the electron plasma frequency. The electron broadening of this part of the line is primarily due to weak electron collisions, so we can well approximate $M(\omega)$ by retaining only second order terms in an expansion in $V_1(r,1)$ (Smith, Cooper, and Vidal 1969). With these approximations we have

$$M(\omega) = nTr_1 L_1(r,1)\left[\omega - L(r) - L(1)\right]^{-1} L_1(r,1)f(1) , \qquad (1.6.4)$$

where

$$f(r) = e^{-\beta H(r)}/Tr_r e^{-\beta H(r)} \qquad (1.6.5)$$

and

$$f(1) = \frac{N}{n} e^{-\beta H(1)}/Tr_1 e^{-\beta H(1)} . \qquad (1.6.6)$$

In Appendix A we discuss the NQA and NLBA, and show that as a consequence of these approximations, $M(\omega)$ has the matrix form (Tighe 1977)

$$M(\omega)_{ii'} =$$

$$-\frac{in}{h^2} Tr_1 \int_o^\infty dt \sum_{i''} e^{i\Delta\omega t} V_{ii''} e^{-iH(1)t/\hbar} V_{i''i'} e^{iH(1)t/\hbar} f(1) , \qquad (1.6.7)$$

where $\Delta\omega = \omega - (E_{i''} - E_f)/\hbar$ and the subscript i (f) represents initial (final) states for the particular Lyman line to be calculated. We will partially include the effects of quenching later in this work.

This form of $M(\omega)$ with the dipole approximation for $V_1(r,1)$ was used by O'Brien (1970) and Tighe (1977) in calculating Lyman line shapes for charged radiators. Here, we will retain the full Coulomb interaction, $V_1(r,1)$, in calculating Lyman series lines.

CHAPTER II

THE FULL COULOMB RADIATOR–PERTURBER INTERACTION

II.1 The Line Width and Shift Operator

The purpose of this chapter is to develop a computational form for

$M(\omega)$ in which we make no approximations for the radiator-perturbing

electron interaction, Eq. (1.6.3). We will calculate matrix elements

of $M(\omega)$ in the spherical representation, $|n\ell m\rangle$, where n is the principal

quantum number of the initial level of a Lyman transition. The perturb-

ing electron Hamiltonian, $H(1)$, is that of a particle in an attractive

Coulomb potential, so we will use the Coulomb wavefunctions to evaluate

the trace in $M(\omega)$ (O'Brien 1970). The eigenfunctions of $H(1)$ are (Alder

et al. 1956)

$$\langle \vec{x} | \vec{k} \rangle = \sum_{\ell m} \frac{4\pi}{(2\pi)^{3/2}} i^\ell e^{i\sigma(\ell,k)} Y^*_{\ell m}(\hat{k}) Y_{\ell m}(\hat{x})(kx)^{-1} F_\ell(\eta,kx)$$

(2.1.1)

where

$$\sigma(\ell,k) = \arg\Gamma(\ell + 1 + i\eta),$$

$$\eta = \frac{-(Z-1)}{k},$$

$F_\ell(\eta,kx)$ is the Coulomb wavefunction (Abramowitz and Stegun 1972):

$$F_\ell(\eta,\rho) = 2^\ell e^{\frac{-\pi\eta}{2}} \frac{|\Gamma(\ell+1+i\eta)|}{\Gamma(2\ell+2)} \rho^{\ell+1} e^{-i\rho} {}_1F_1(\ell+1+i\eta,2\ell+2,2i\rho),$$

(2.1.2)

17

and $_1F_1$ is the confluent hypergeometric function. The energy
eigenvalues of H(1) are given by

$$H(1)\,|\vec{k}\rangle = \frac{\hbar^2 k^2}{2m}\,|\vec{k}\rangle \ . \qquad (2.1.3)$$

With these functions we write the radiator matrix elements
of $M(\omega)$ (Eq. 1.6.7) as

$$M(\omega)_{n\ell_1 m_1 mn\ell_2 m_2} = -\,\frac{i n_e \lambda_T^{\ 3}}{h^2}\int_0^\infty dt\ e^{i\Delta\omega t}$$

$$\times \sum_{\ell_3 m_3}\ \int d\vec{k}_1 \int d\vec{k}_2\ \langle \vec{k}_1 n\ell_1 m_1|V_1(r,1)|\vec{k}_2 n\ell_3 m_3\rangle$$

$$\times \langle \vec{k}_2 n\ell_3 m_3|\ e^{-iH(1)t/h}V_1(r,1)e^{iH(1)t/h}e^{-\beta H(1)}|\vec{k}_1 n\ell_2 m_2\rangle, \quad (2.1.4)$$

where n_e is the perturbing electron density and λ_T is the thermal
wavelength,

$$\lambda_T = \big(\frac{2\pi\beta\hbar^2}{m}\big)^{1/2} \ .$$

The ket $|\vec{k}n\ell m\rangle$ is the product of perturber and radiator kets,
$|\vec{k}\rangle|n\ell m\rangle$. From Eq. (2.1.1) we see that the k-angle dependence of the
perturber wavefunction $\langle\vec{x}|\vec{k}\rangle$ can be written explicitly as

$$\langle\vec{x}|\vec{k}\rangle = \sum_{\ell=0}^\infty\ \sum_{m=-\ell}^\ell Y^*_{\ell m}(\hat{k})\langle\vec{x}|k\ell m\rangle \ . \qquad (2.1.5)$$

We use this in the expression for $M(\omega)$, obtaining four ℓ,m-sums over
perturber angular momenta. The k_1- and k_2-angle integrals each are

integrals of two spherical harmonics. These can be done to obtain Kronecker deltas which reduce the four ℓ,m-sums to two, which we label ℓ_4,m_4 and ℓ_6,m_6. We then have

$$M(\omega)_{n\ell_1 m_1, n\ell_2 m_2} = -\frac{1}{\hbar^2} \int_o^\infty dt \; e^{i\Delta\omega t} \int_o^\infty dk_1 \int_o^\infty dk_2$$

$$\times \; e^{\frac{i\hbar}{2m}(k_1^2 - k_2^2)t} \; e^{-\frac{\beta\hbar^2 k_1^2}{2m}} \; G_{n\ell_1 m_1, n\ell_2 m_2}(k_1, k_2) \qquad (2.1.6)$$

where

$$G_{n\ell_1 m_1, n\ell_2 m_2}(k_1, k_2) = n_e \lambda_T^3 k_1^2 k_2^2 \sum_{\ell_3 m_3} \sum_{\ell_4 m_4} \sum_{\ell_6 m_6}$$

$$\times \; \langle k_1 \ell_4 m_4 n\ell_1 m_1 | V_1(r,1) | k_2 \ell_6 m_6 n\ell_3 m_3 \rangle$$

$$\times \; \langle k_2 \ell_6 m_6 n\ell_3 m_3 | V_1(r,1) | k_1 \ell_4 m_4 n\ell_2 m_2 \rangle \; . \qquad (2.1.7)$$

In Appendix B we reduce $G(k_1, k_2)$ to the form

$$G_{n\ell_1 m_1, n\ell_2 m_2}(k_1, k_2) = \frac{4 n_e \lambda_T^3 e^4}{\pi^2} \; \delta_{\ell_1 \ell_2} \delta_{m_1 m_2} \sum_{\ell_3=0}^{n-1} \sum_{\ell_5=0}^{2n-2} \sum_{\ell_4, \ell_6=0}^{\infty}$$

$$\times \; \frac{(2\ell_3+1)(2\ell_4+1)(2\ell_6+1)}{(2\ell_5+1)} \begin{pmatrix} \ell_1 & \ell_3 & \ell_5 \\ 0 & 0 & 0 \end{pmatrix}^2 \begin{pmatrix} \ell_4 & \ell_5 & \ell_6 \\ 0 & 0 & 0 \end{pmatrix}^2$$

$$\times \; \left[\int_o^\infty dx \; F_{\ell_4}(\eta_1, k_1 x) F_{\ell_6}(\eta_2, k_2 x) A_{\ell_1 \ell_3 \ell_5}(x) \right]^2 \; , \qquad (2.1.8)$$

where

$$A_{\ell_1 \ell_3 \ell_5}(x) = \int_o^\infty dx_r x_r^2 \; R_{n\ell_1}(x_r) \left(\frac{x_<^{\ell_5}}{\ell_5+1} - \frac{\delta_{\ell_5,0}}{x} \right) R_{n\ell_3}(x_r) \; , \qquad (2.1.9)$$

$R_{n\ell}(x_r)$ is the hydrogenic radial wavefunction of the radiator, and $x_<$ ($x_>$) is the lesser (greater) of x_r and x, the radial coordinates of the radiator electron and perturbing electron. The ℓ_3 sum is over initial radiator angular momenta, the ℓ_5 sum is over multipoles of the Coulomb interaction, and the ℓ_4 and ℓ_6 sums are over perturber angular momenta. The symbol

$$
\begin{pmatrix} \ell_1 & \ell_2 & \ell_3 \\ m_1 & m_2 & m_3 \end{pmatrix}
$$

is the Wigner 3-j symbol (Edmonds 1957). In Appendix C we express $A_{\ell_1 \ell_3 \ell_5}(x)$ as a sum which is convenient for numerical evaluation.

The time integration in $M(\omega)$ (Eq. 2.1.6) can be done by adding the convergence factor $i\varepsilon$ ($\varepsilon>0$) to $\Delta\omega$, then taking the limit as $\varepsilon\to 0$:

$$
\lim_{\varepsilon\to 0} \int_0^\infty dt \; e^{i(\Delta\omega+i\varepsilon)t} \; e^{\frac{i\hbar}{2m}(k_1^2 - k_2^2)t} =
$$

$$
= \lim_{\varepsilon\to 0} \frac{i}{\Delta\omega + \frac{\hbar}{2m}(k_1^2 - k_2^2) + i\varepsilon}
$$

$$
= P\frac{i}{\Delta\omega + \frac{\hbar}{2m}(k_1^2 - k_2^2)} + \pi\delta(\Delta\omega + \frac{\hbar}{2m}(k_1^2 - k_2^2)), \qquad (2.1.10)
$$

where P stands for the Cauchy principal part. This separates $M(\omega)$ into real and imaginary parts,

$$
M_R(\Delta\omega) = \frac{1}{\hbar^2} P \int_0^\infty dk_1 \int_0^\infty dk_2 \; \frac{e^{-\frac{\beta\hbar^2 k_1^2}{2m}} G(k_1,k_2)}{\Delta\omega + \frac{\hbar}{2m}(k_1^2 - k_2^2)} , \qquad (2.1.11)
$$

and

$$
M_I(\Delta\omega) = -\frac{m\pi}{\hbar^3} \int_0^\infty dk_1 \; e^{-\frac{\beta\hbar^2 k_1^2}{2m}} \; \frac{G\left(k_1, (k_1^2 + \frac{2m\Delta\omega}{\hbar})^{1/2}\right)}{(k_1^2 + \frac{2m\Delta\omega}{\hbar})^{1/2}} , \quad \Delta\omega>0;
$$
$$
(2.1.12)
$$

$$M_I(\Delta\omega) = e^{-\beta\hbar|\Delta\omega|} M_I(|\Delta\omega|), \quad \Delta\omega<0. \tag{2.1.13}$$

The function $M_R(\Delta\omega)$ represents a dynamic shift of the spectral line due to the interaction of the radiator with the perturbing electrons of the plasma, $M_I(\Delta\omega)$ represents the width of the line due to the perturbing electrons. We use the fact that (O'Brien and Hooper 1974)

$$P \int_o^\infty dk_2 \, e^{-\frac{\beta\hbar^2 k_1^2}{2m}} \frac{G\left(k_1,(k_1^2 + \frac{2m\Delta\omega}{\hbar})^{1/2}\right)}{\Delta\omega + \frac{\hbar}{2m}(k_1^2 - k_2^2)} = 0, \quad \Delta\omega>0,$$

to write $M_R(\Delta\omega)$ in the form

$$M_R(\Delta\omega) =$$

$$\frac{1}{\hbar^2} \int_o^\infty dk_1 \int_o^\infty dk_2 \, e^{-\frac{\beta\hbar^2 k_1^2}{2m}} \frac{\left[G(k_1,k_2) - G\left(k_1,(k_1^2 + \frac{2m\Delta\omega}{\hbar})^{1/2}\right)\right]}{\Delta\omega + \frac{\hbar}{2m}(k_1^2 - k_2^2)}, \quad \Delta\omega>0. \tag{2.1.14}$$

This integrand is not divergent so the principal part notation is not necessary. Similarly, for $\Delta\omega<0$,

$$M_R(\Delta\omega) = \frac{1}{\hbar^2} \int_o^\infty dk_1 \int_o^\infty dk_2$$

$$\times \frac{\left[e^{-\frac{\beta\hbar^2 k_1^2}{2m}} G(k_1,k_2) - e^{-\beta\left(\frac{\hbar^2 k_2^2}{2m} + \hbar|\Delta\omega|\right)} G\left((k_2^2 + \frac{2m|\Delta\omega|}{\hbar})^{1/2},k_2\right)\right]}{\Delta\omega + \frac{\hbar}{2m}(k_1^2 - k_2^2)}. \tag{2.1.15}$$

Equations (2.1.12)-(2.1.15) for $M_R(\Delta\omega)$ and $M_I(\Delta\omega)$ are evaluated numerically and the results are used in Eqs. (1.5.19) and (1.4.13) to generate line shapes. We will present the results of these calculations in Chapter III.

II.2   Angular Momentum Sums

The function $G(k_1,k_2)$, which appears in Eqs. (2.1.12)-(2.1.15) for $M(\omega)$, contains infinite sums over the perturber angular momenta, ℓ_4 and ℓ_6. Increasing ℓ values in these sums correspond to increasing separation of the radiator and perturber, so for ℓ_4 and ℓ_6 greater than some value, say ℓ', we can use the dipole approximation for the radiator-perturber interaction with negligible error. The part of the sum in which the dipole approximation is used can then be summed exactly.

We separate $G(k_1,k_2)$ into two parts,

$$G(k_1,k_2) = G^{(1)}(k_1,k_2) + G^{(2)}(k_1,k_2), \qquad (2.2.1)$$

where $G^{(1)}$ is to be calculated numerically from Eq. (2.1.8) with the upper bound ℓ' on the ℓ_4 and ℓ_6 sums, and $G^{(2)}$ is to be calculated from a dipole approximation of Eq. (2.1.8) for the remainder of the ℓ_4 and ℓ_6 sums. The dipole approximation for Eq. (2.1.8) is obtained by restricting the ℓ_5 sum to the dipole term, $\ell_5 = 1$, and replacing Eq. (2.1.9) for $A_{\ell_1\ell_3\ell_5}(x)$ by

$$A^d_{\ell_1\ell_3}(x) = \frac{1}{x^2} \int_0^\infty dx_r x_r^3 R_{n\ell_1}(x_r)R_{n\ell_3}(x_r)$$

$$= \frac{3na_o}{2Zx^2}\left[(n^2-\ell_1^2)^{1/2} \delta_{\ell_1,\ell_3+1} + (n^2 - (\ell_1+1))^{1/2}\delta_{\ell_1,\ell_3-1} \right] . \qquad (2.2.2)$$

We obtain this last expression from $A_{\ell_1 \ell_3 \ell_5}(x)$ by replacing $x_</x_>^2$ with x_r/x^2, which is consistent with the assumption that the perturber is far from the radiator. Since $\ell_5 = 1$ in $G^{(2)}$, we can use the equation (Edmonds 1957)

$$\begin{pmatrix} \ell & \ell+1 & 1 \\ 0 & 0 & 0 \end{pmatrix} = (-1)^{\ell-1} \left[\frac{(\ell+1)}{(2\ell+3)(2\ell+1)} \right]^{1/2} \qquad (2.2.3)$$

to evaluate the 3-j symbols in $G^{(2)}$; then we sum over ℓ_3 to obtain

$$G^{(2)}_{n\ell_1 m_1, n\ell_2 m_2}(k_1, k_2) =$$

$$\frac{4n_e \lambda_T^3 e^4}{3\pi^2} \left(\frac{3na_o}{2Z}\right)^2 \delta_{\ell_1 \ell_2} \delta_{m_1 m_2} (n^2 - \ell_1^2 - \ell_1 - 1) f_{\ell'}(k_1, k_2) \qquad (2.2.4)$$

where

$$f_{\ell'}(k_1, k_2) = \sum_{\ell=\ell'+1}^{\infty} \ell \left\{ \left[\int_o^\infty dx F_{\ell-1}(\eta_1, k_1 x) F_\ell(\eta_2, k_2 x) \frac{1}{x^2} \right]^2 \right.$$

$$\left. + \left[\int_o^\infty dx F_\ell(\eta_1, k_1 x) F_{\ell-1}(\eta_2, k_2 x) \frac{1}{x^2} \right]^2 \right\} . \qquad (2.2.5)$$

The ℓ-sum in this equation can be done analytically (Biedenharn 1956) with the result

$$f_{\ell'}(k_1, k_2) = \ell'\left(k_1^2 + k_2^2 + \frac{2k_1^2 \eta_1^2}{\ell'^2}\right) \left[\int_o^\infty dx \; x^{-1} F_{\ell'-1}(\eta_1, k_1 x) F_{\ell'-1}(\eta_2, k_2 x) \right]^2$$

$$-2\ell' k_1 k_2 \left| 1 + \frac{i\eta_1}{\ell'} \right| \left| 1 + \frac{i\eta_2}{\ell'} \right| \left[\int_o^\infty dx \; x^{-1} F_{\ell'}(\eta_1, k_1 x) F_{\ell'}(\eta_2, k_2 x) \right]$$

$$\times \left[\int_o^\infty dx \; x^{-1} F_{\ell'-1}(\eta_1, k_1 x) F_{\ell'-1}(\eta_2, k_2 x) \right] . \qquad (2.2.6)$$

If we set ℓ' equal to one in $G^{(2)}$, we obtain the dipole form of
$M(\omega)$ used by O'Brien (1970) and Tighe (1977). O'Brien showed that
$f_1(k_1,k_2)$ is related to the free-free Gaunt factor, $g(k_1,k_2)$, by

$$f_1(k_1,k_2) = \frac{\pi}{2\sqrt{3}} \, k_1 k_2 g(k_1,k_2).$$

Karzas and Latter (1961) and O'Brien (1970,1971) have calculated the
free-free Gaunt factor numerically. They reduce the integrals in
$g(k_1,k_2)$ to sums which are convenient for computer evaluation. The work
of O'Brien, which was for singly ionized helium, was extended by Tighe
to radiators of arbitrary charge. We extend their work to evaluate
$f_{\ell'}(k_1,k_2)$ for $\ell'>1$. We use this in Eq. (2.2.4) to obtain $G^{(2)}$; then we
calculate $M(\omega)$ from $G = G^{(1)} + G^{(2)}$ according to Eqs. (2.1.12)-(2.1.15).
We calculate $M(\omega)$ for increasing values of ℓ' to determine when the
dipole approximation in $G^{(2)}$ gives negligible error, i.e. when $M(\omega)$
becomes independent of ℓ'.

II.3 Electron Correlations

In calculating Eqs. (2.1.12) - (2.1.15) for $M_I(\Delta\omega)$ and $M_R(\Delta\omega)$, we
used the approximation that the perturbing electrons do not interact
with each other, thereby removing effects due to electron-electron
correlations. Here we reintroduce in an approximate manner the effect
of these correlations on the line shape.

These correlations have been shown to produce a screening of the
radiator-perturbing electron interaction (Hussey et al. 1977). This
screening is most significant for the part of the line shape
corresponding to times which are long compared to electron relaxation

times, that is, for frequencies inside the electron plasma frequency.
Smith (1968) and Hussey et al. (1977) show that the inclusion of corre-
lations has little effect on $M_I(\Delta\omega)$ for $|\Delta\omega| > \omega_{pe}$ and that for
$|\Delta\omega| < \omega_{pe}$ the result for $M_I(\Delta\omega)$ including correlations is nearly equal
to the uncorrelated result evaluated at the plasma frequency, $M_I(\omega_{pe})$.
Hence, to approximate the effects of correlations on $M_I(\Delta\omega)$, we set
$M_I(\Delta\omega) = M_I(\omega_{pe})$ for $|\Delta\omega| < \omega_{pe}$.

To approximately include electron correlation effects in $M_R(\Delta\omega)$ we
replace the Coulomb interaction $V_1(r,1)$ in $G(k_1,k_2)$ (Eq. 2.1.7) by the
Debye-screened interaction $V_1(r,1)e^{-x_1/\lambda_D}$; then use the screened
$G(k_1,k_2)$ in calculating Eqs. (2.1.14) and (2.1.15) for $M_R(\Delta\omega)$. This
approximate treatment of correlations follows from a calculation by
Dufty and Boercker (1976), based on a ring approximation treatment of
electron-electron interactions (Brout and Caruthers 1963), in which they
obtain a fully screened form for $M(\omega)$,

$$M(\omega) = nTr_1 \mathcal{L}(r,1;\Delta\omega)f(r1)[\Delta\omega - L(1) - \mathcal{L}(r1)]^{-1} \times \mathcal{L}(r1)f(r)^{-1},$$

$$(2.3.1)$$

where $\mathcal{L}(r,1;\Delta\omega)$ is a dynamically screened radiator-perturbing electron
interaction. Then they proceed to show that for $\Delta\omega << \omega_{pe}$ and in the
non-degenerate limit, the radiator-perturber interactions can be written
in the Debye-screened form

$$V_s(r,1) = \frac{e^2}{|\vec{x}_1-\vec{x}_r|} e^{-|\vec{x}_1-\vec{x}_r|/\lambda_D} - \frac{e^2}{x_1} e^{-x_1/\lambda_D} . \qquad (2.3.2)$$

For the plasma conditions which we will consider, λ_D is significantly
larger than the radiator size so we approximate Eq. (2.3.2) by

$$V_s(r,1) \cong V_1(r,1) \ e^{-x_1/\lambda_D} \ . \qquad (2.3.3)$$

Then, using the approximations of Section I.6 (except for the neglect of electron correlations), we can write Eq. (2.3.1) as

$$M(\omega) = nTr_1 V_s(r,1)[\Delta\omega - L(1)]^{-1} V_s(r,1)f(1) \ . \qquad (2.3.4)$$

This is the same as Eq. (1.6.7) except for the screened interactions. Following the steps specified in Section II.1 we can obtain from Eq. (2.3.4) the Equations (2.1.14) and (2.1.15) for $M_R(\Delta\omega)$, except that $G(k_1,k_2)$ will contain the screened interaction, Eq. (2.3.3).

II.4 Interaction Matrix Elements Between States of Different Principal Quantum Number

So far we have assumed that matrix elements of the radiator-perturber interactions between radiator states having different principal quantum numbers are negligible and have set them equal to zero (see Appendix A). With these approximations and the No Lower State Broadening Approximation, the calculation of a Lyman line shape involves matrices which have rows and columns labeled by the initial radiator states of the line. By using these approximations we have neglected quenching, or radiationless transitions between radiator states of different principal quantum number caused by the perturbing electrons. We have also neglected Stark shifts of higher then first order in the ion microfield and the changed oscillator strengths due to mixing of radiator states of different principal quantum number by the ion microfield.

For a given line we expect that the most significant of the neglected matrix elements are those between the initial states of a given spectral line (principal quantum number = n) and the states of the nearest adjacent energy level (principal quantum number = n+1). Here we will include these matrix elements in the calculation of the n→1 Lyman line shape. The matrices involved in this calculation will have rows and columns labeled by radiator states of principal quantum number n and n+1. We write Eq. (1.5.19) for $J(\omega,\varepsilon)$ in the matrix form

$$J(\omega,\varepsilon) = -\frac{1}{\pi} \, \text{Im} \sum_{ii'} \vec{d}_{1i} \cdot \left[\omega - (H(r)/\hbar - \omega_1) - M(\omega)\right]^{-1}_{ii'} f_i \, \vec{d}_{i'1}, \qquad (2.4.1)$$

where $H(r)$ is the Hamiltonian for the radiator in the presence of the ion microfield ε, $\hbar\omega_1$ is the energy of the radiator ground state, and i, i' represent radiator states having principal quantum numbers n or n+1. We will neglect the line shift, so in Eq. (2.4.1) we have set B=0, and we will set $M_R(\omega) = 0$.

Following the derivation of Eqs. (2.1.6) and (2.1.8) from Eq. (1.6.7) we can write $M(\omega)_{ii'}$ as

$$M(\omega)_{n_1 \ell_1 m_1, n_2 \ell_2 m_2} = -\frac{i}{\hbar^2} \sum_{n_3 \ell_3} \int_0^\infty dt e^{i\Delta\omega_{n_3 1} t} \int_0^\infty dk_1 \int_0^\infty dk_2$$

$$\times \, e^{\frac{i\hbar}{2m}(k_1^2 - k_2^2)t} \, e^{-\frac{\beta \hbar^2 k_1^2}{2m}} \, G_{n_1 \ell_1 m_1, n_2 \ell_2 m_2, n_3 \ell_3}(k_1, k_2) \qquad (2.4.2)$$

where $\Delta\omega_{n_3 1} = \omega - (\omega_{n_3} - \omega_1) = \omega - \omega_{n_3 1}$, $\hbar\omega_{n_3}$ is the unperturbed energy of the states with principal quantum number n_3. Here, the principal quantum numbers n_1, n_2, and n_3 can have the values n and n+1. The term $G(k_1, k_2)$ is given by

$$G_{n_1 \ell_1 m_1, n_2 \ell_2 m_2, n_3 \ell_3}(k_1, k_2) = \frac{4 n e \lambda_T^3 e^4}{\pi^2} \delta_{\ell_1 \ell_2} \delta_{m_1 m_2} \sum_{\ell_5=0}^{2n} \sum_{\ell_4, \ell_6=0}^{\infty}$$

$$\times \frac{(2\ell_3+1)(2\ell_4+1)(2\ell_6+1)}{(2\ell_5+1)} \begin{pmatrix} \ell_1 & \ell_3 & \ell_5 \\ 0 & 0 & 0 \end{pmatrix}^2 \begin{pmatrix} \ell_4 & \ell_5 & \ell_6 \\ 0 & 0 & 0 \end{pmatrix}^2$$

$$\times \int_0^{\infty} F_{\ell_4}(\eta_1, k_1 x) F_{\ell_6}(\eta_2, k_2 x) A_{n_1 n_3 \ell_1 \ell_3 \ell_5}(x) dx$$

$$\times \int_0^{\infty} F_{\ell_4}(\eta_1, k_1 x) F_{\ell_6}(\eta_2, k_2 x) A_{n_2 n_3 \ell_1 \ell_3 \ell_5}(x) dx . \qquad (2.4.3)$$

The term $A(x)$ is given by

$$A_{n_1 n_3 \ell_1 \ell_3 \ell_5}(x) = \int_0^{\infty} dx_r x_r^2 R_{n_1 \ell_1}(x_r) \left(\frac{x_<^{\ell_5}}{x_>^{\ell_5+1}} - \frac{\delta_{\ell_5,0}}{x} \right) R_{n_3 \ell_3}(x_r) . \qquad (2.4.4)$$

We use Eq. (2.1.10) to do the time integration in Eq. (2.4.2) for $M(\omega)$, obtaining for the imaginary part of $M(\omega)$:

$$M_I(\omega)_{n_1 \ell_1 m_1, n_2 \ell_2 m_2} = -\frac{\pi}{\hbar^2} \sum_{n_3 \ell_3} \int_0^{\infty} dk_1 \int_0^{\infty} dk_2 \, e^{-\frac{\beta \hbar^2 k_1^2}{2m}}$$

$$\times G_{n_1 \ell_1 m_1, n_2 \ell_2 m_2, n_3 \ell_3}(k_1, k_2) \delta\left(\Delta\omega_{n_3 1} - \frac{\hbar^2}{2m}(k_2^2 - k_1^2) \right) . \qquad (2.4.5)$$

We rewrite $\Delta\omega_{n_3 1}$ as $\Delta\omega_{n_3 1} = \Delta\omega - \omega_{n_3 n}$, where $\Delta\omega$ is the frequency separation from the unperturbed line center, $\Delta\omega = \omega - \omega_{n1}$. Then we do one of the k-integrations to obtain

$$M_I(\Delta\omega)_{n_1\ell_1 m_1, n_2\ell_2 m_2} =$$

$$-\frac{m\pi}{\hbar^3}\left[\sum_{\ell_3=1}^{n-1}\int_o^\infty dk_1\, e^{-\frac{\beta\hbar^2 k_1^2}{2m}}\,\frac{G_{n_1\ell_1 m_1, n_2\ell_2 m_2, n_3\ell_3}(k_1,(k_1^2+\frac{2m\Delta\omega}{\hbar})^{1/2})}{(k_1^2+\frac{2m\Delta\omega}{\hbar})^{1/2}}\right.$$

$$+\sum_{\ell_3=0}^{n}\int_o^\infty dk_2 e^{-\frac{\beta\hbar^2}{2m}(k_2^2+\frac{2m}{\hbar}(\omega'-\Delta\omega))}$$

$$\left.\times\,\frac{G_{n_1\ell_1 m_1, n_2\ell_2 m_2, n_3\ell_3}((k_2^2+\frac{2m}{\hbar}(\omega'-\Delta\omega))^{1/2},k_2)}{(k_2^2+\frac{2m}{\hbar}(\omega'-\Delta\omega))^{1/2}}\right], \qquad \Delta\omega>0; \quad (2.4.6)$$

$$M_I(\Delta\omega)_{n_1\ell_1 m_1, n_2\ell_2 m_2} =$$

$$-\frac{m\pi}{\hbar^3}\left[\sum_{\ell_3=0}^{n-1}\int_o^\infty dk_2 e^{-\beta\hbar|\Delta\omega|-\frac{\beta\hbar^2 k_2^2}{2m}}\,G_{n_1\ell_1 m_1, n_2\ell_2 m_2, n_3\ell_3}((k_2^2+\frac{2m}{\hbar}|\Delta\omega|)^{1/2},k^2)\right.$$

$$\left.+\text{ (second term of Eq. (2.4.6))}\right], \qquad \Delta\omega<0; \qquad (2.4.7)$$

where $\omega' = \omega_{n+1,n}$. Here we have broken the n_3-sum into two parts: the first term in the brackets of Eqs. (2.4.6) and (2.4.7) is for $n_3=n$; the second is for $n_3=n+1$. We evaluate Eqs. (2.4.6) and (2.4.7) numerically; then use these results in Eqs. (2.4.1) and (1.4.13) to obtain line shapes. Results of this calculation are presented in Section III.2.

CHAPTER III
RESULTS

III.1 Symmetric Line Profiles

Here we compare the results generated using this full Coulomb
version of the relaxation theory with those results from the relaxation
theory in which the dipole approximation is made for the radiator-
perturbing electron interaction (Tighe 1977; Tighe and Hooper 1976,
1978). We will also examine the relative importance of various multi-
poles of the Coulomb interaction in $M_I(\Delta\omega)$ by restricting the ℓ_5-sum in
Eq. (2.1.8) to the multipoles of interest. In this section we will
neglect the line shift, which is given by the terms B and $M_R(\Delta\omega)$, and
consider only the broadening effects of the electrons, given by $M_I(\Delta\omega)$
(Eqs. 2.1.12 and 2.1.13). We will examine line shifts and asymmetries
in section III.2.

Comparison of Coulomb and Dipole Results

In Figures 1 and 2 we compare Lyman α and β line profiles calcu-
lated from this full Coulomb formalism with profiles in which the dipole
approximation was used. The lines appearing in these figures were
calculated for a plasma of Ar^{+17} ions and electrons at a density of 10^{24}
electrons per cubic centimeter and a temperature of 800 eV, conditions
which approximate the plasmas of some recent laser implosion experiments
(Yaakobi et al. 1980). For the Lyman α lines presented here, the
neglected fine structure splitting of about 0.35 Ryd. would have a

30

Figure 1   Comparison of an Argon Lyman α line profile calculated from
            the full Coulomb interaction with the corresponding profile
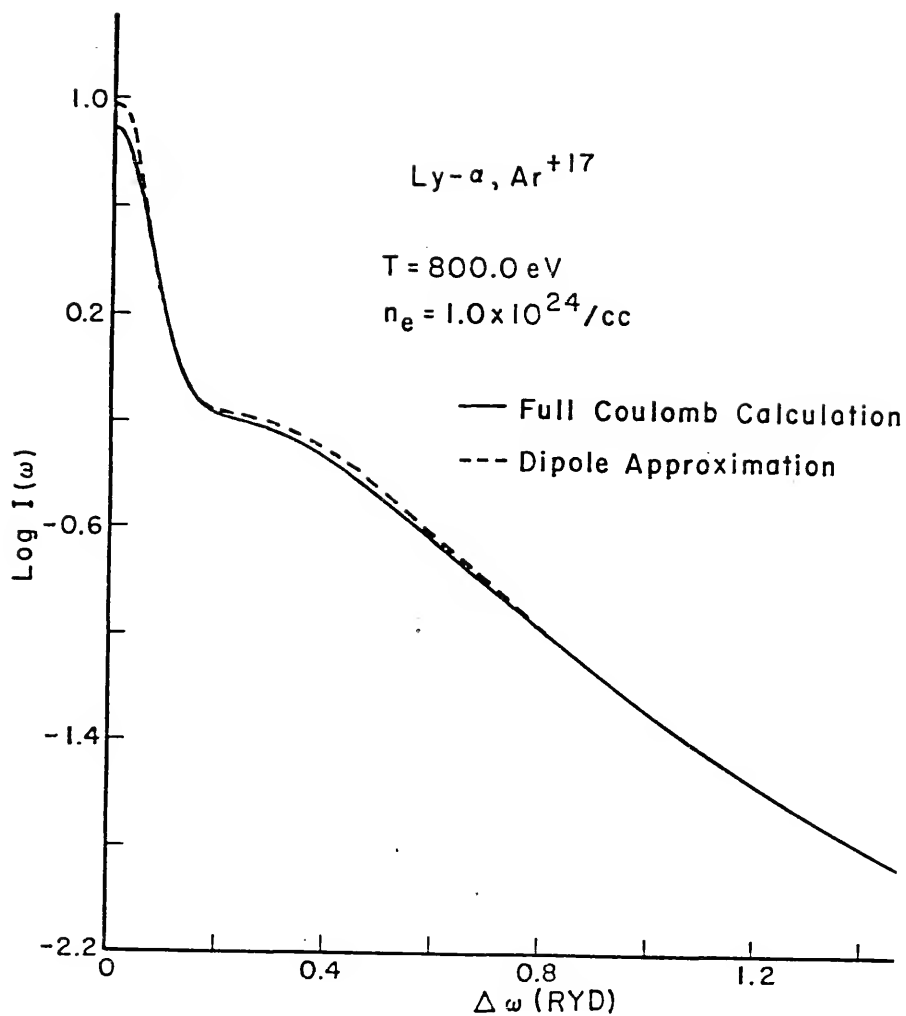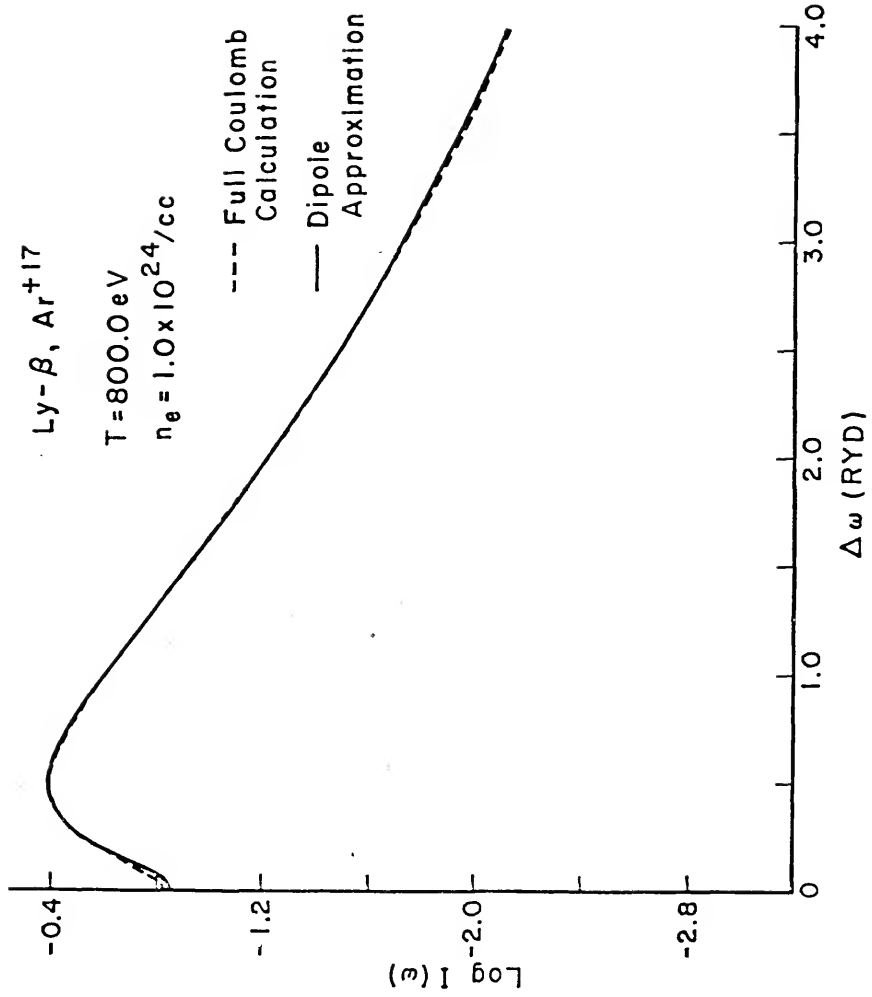   calculated from the dipole approximation for that
            interaction.

$Ly-\alpha$, Ar^{+17}

$T = 800.0 \, eV$
$n_e = 1.0 \times 10^{24}/cc$

—— Full Coulomb Calculation
--- Dipole Approximation

Figure 2   Comparison of an Argon Lyman β line profile calculated from
            the full Coulomb interaction with the corresponding profile
            calculated from the dipole approximation for that
            interaction.

Ly-β, Ar^{+17}

T = 800.0 eV

n_e = 1.0x10^{24}/cc

- - - Full Coulomb
     Calculation

—— Dipole
     Approximation

$\Delta \omega$ (RYD)

Log I (ω)

noticeable effect on the lines (Lee 1979), but this should be negligible in the case of the β lines. Figure 1 shows a slightly broader central peak for the α line calculated from the Coulomb interaction than for the α line calculated from the dipole approximation. In Figure 2 the β line from the Coulomb calculation has a slightly less pronounced central depression than does the corresponding dipole line. The Coulomb and dipole calculations show little difference, but this agreement is partly fortuitous. Although the dipole approximation of the Coulomb interaction neglects broadening due to the other multipoles of the interaction, it overestimates the dipole ($\ell_5=1$) part of the Coulomb interaction for perturbers which are less than a few times the average radiator diameter from the radiator. This nearly compensates for the multipoles neglected in that approximation. Figures 3 and 4 show that Lyman α and β lines calculated from the dipole approximation are significantly broader than those calculated from the dipole part of the Coulomb interaction.

Although we have removed the long range monopole from $V_1(r,1)$ (Eq. 1.6.2), the multipole expansion of $V_1(r,1)$ still contains a monopole contribution from the part of the perturber wavefunction which corresponds to penetration of the radiator, as can be seen from Eq. (C2). If we compare α and β lines calculated from the full Coulomb interaction with lines calculated using the monopole plus dipole part of the Coulomb interaction, the lines from the full Coulomb calculation are only slightly broader, indicating that for these conditions the most significant broadening of these lines is due to the monopole and dipole parts of the interaction.

Figure 3   Comparison of an Argon Lyman α line profile calculated from
the dipole part of the full Coulomb interaction with the
corresponding profile calculated from the dipole
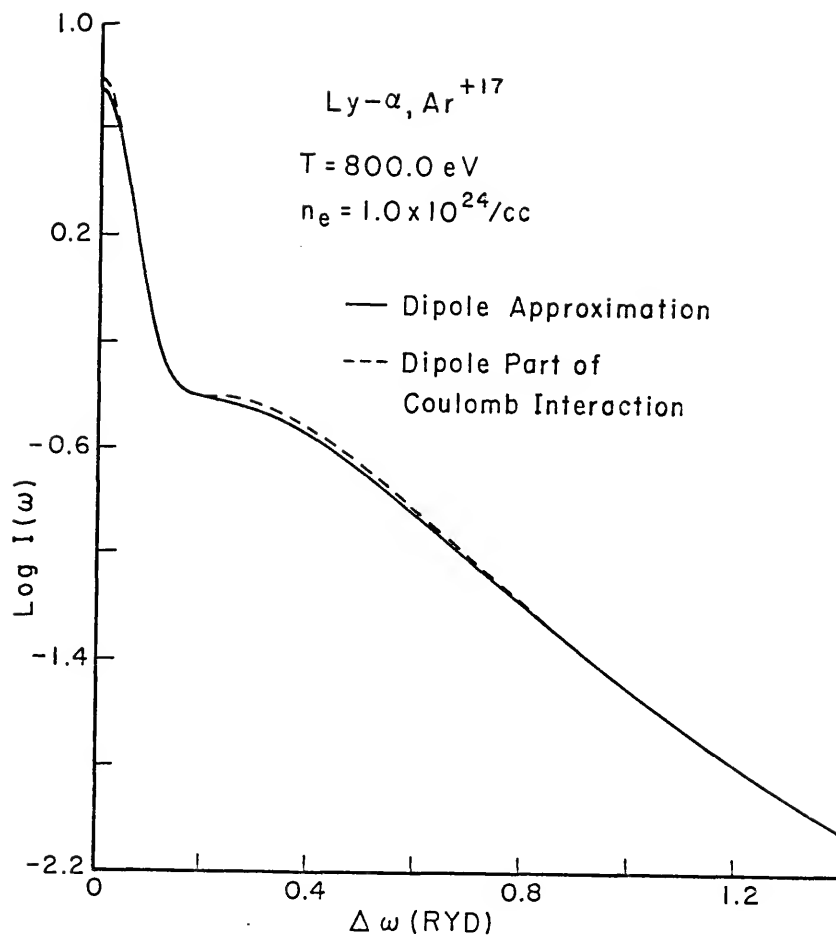approximation for the full Coulomb interaction.

.

$Ly-\alpha, Ar^{+17}$

$T = 800.0 \, eV$

$n_e = 1.0 \times 10^{24}/cc$

—— Dipole Approximation

- - - Dipole Part of Coulomb Interaction

Figure 4   Comparison of an Argon Lyman β line profile calculated from
the dipole part of the full Coulomb interaction with the
corresponding profile calculated from the dipole
approximation for the full Coulomb interaction.

Ly-β, Ar^{+17}

T = 800.0 eV
n_e = 1.0 × 10^{24}/cc

—— Dipole Approximation

--- Dipole Part of Coulomb
        Interaction
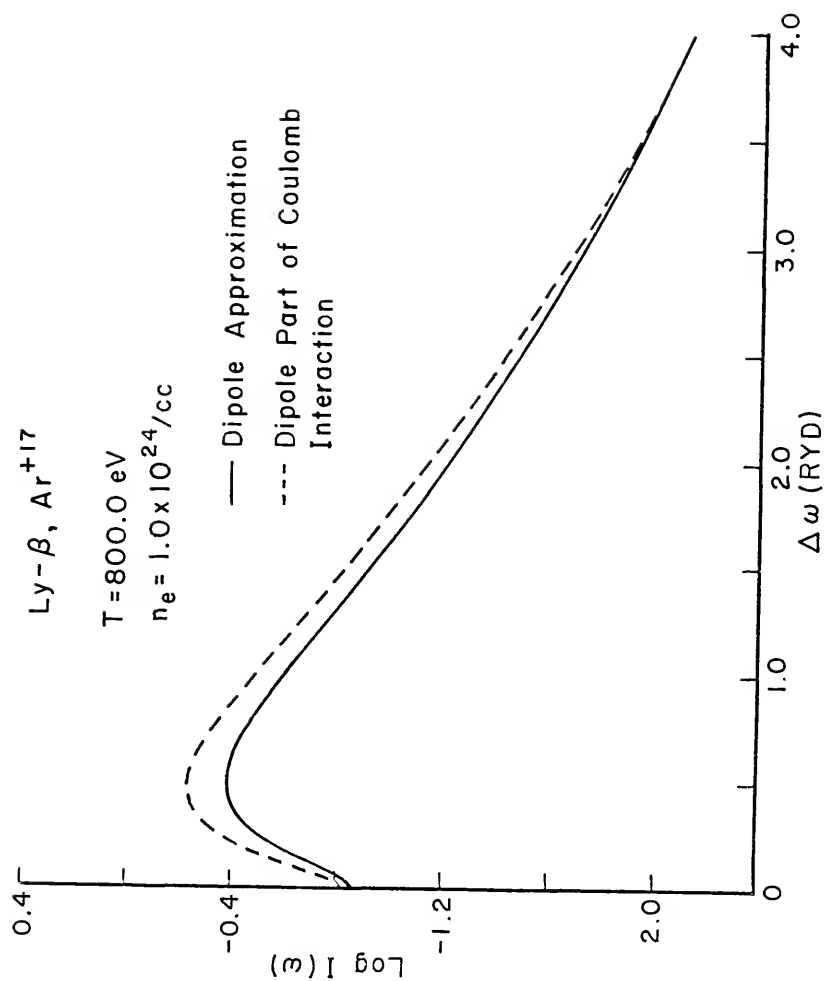
Comparison with Impact Theory

In Figures 5 and 6 we compare line shapes calculated from this full Coulomb relaxation theory to line shapes calculated from a full Coulomb impact theory (Griem et al. 1979; Kepple 1980). This impact calculation approximately accounts for the screening of electron fields and the finite duration of perturbing electron collisions through an appropriate choice of cutoffs of the electron impact parameter. Griem et al. also include, by an approximate method based on partial wave scattering cross sections, the quantum mechanical effects of strong electron-radiator collisions. Figures 5 and 6 show that our α and β lines are slightly broader than those of Griem et al. In Figure 7 we compare our result for a β line at a density of 8.2×10^{23} electrons/cm^3 and a temperature of 800 eV to the results of Griem et al. at 10^{24} electrons/cm^3 and 800 eV. We obtain close agreement on the line wings, the part of the line which we believe to be the most reliable for experimental density determination. Hence, in this range of plasma conditions our calculation would indicate a plasma density about 18% lower than would the calculation of Griem et al.

III.2 Shifts and Asymmetries

So far we have neglected sources of asymmetry in the line profiles. In this section we will examine two significant sources of line asymmetry: the line shift due to perturbing electrons and radiator-perturber interaction matrix elements between states of different principal quantum number.

Figure 5   Comparison of an Argon Lyman α line profile calculated from
          this full Coulomb formalism with an α line profile calculated
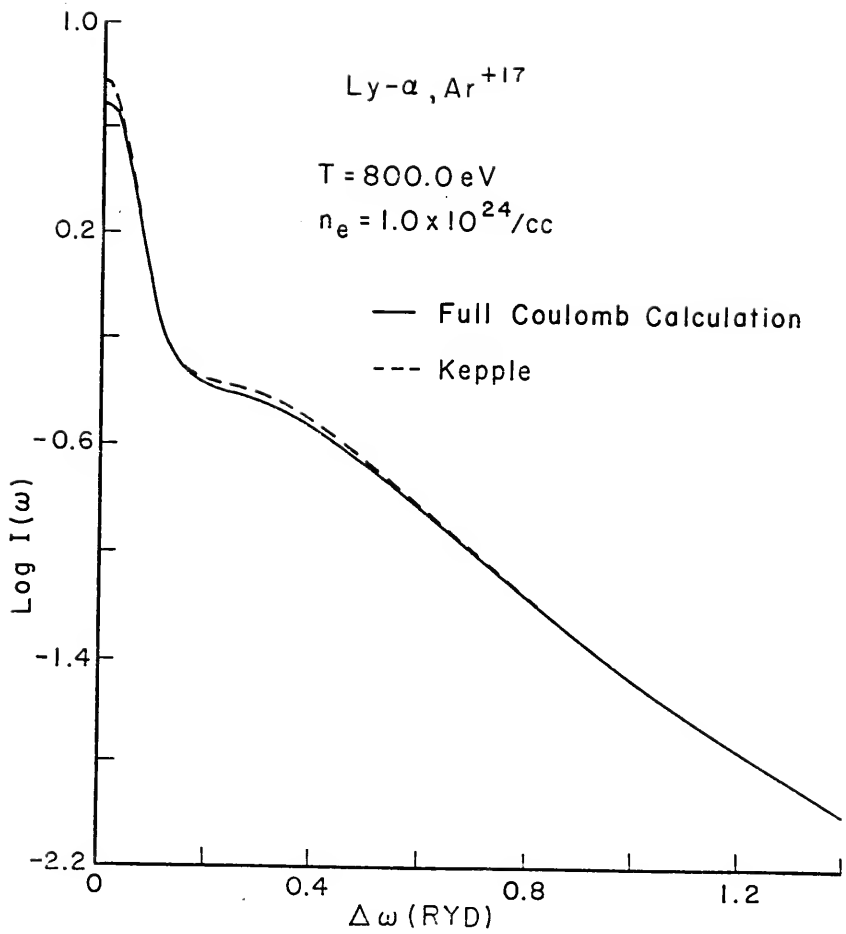   from the full Coulomb impact formalism of Griem, Blaha, and
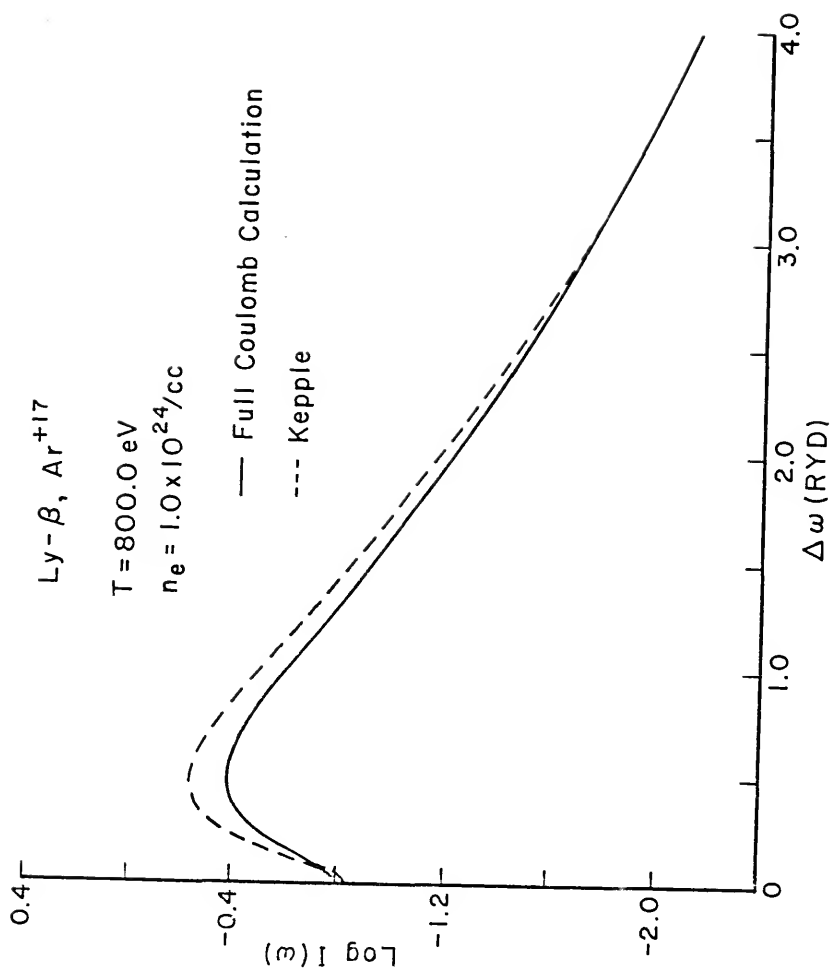   Kepple .

$Ly-\alpha$, Ar^{+17}

$T = 800.0 \, eV$

$n_e = 1.0 \times 10^{24}/cc$

—— Full Coulomb Calculation

--- Kepple

Figure 6   Comparison of an Argon Lyman β line profile calculated from this full Coulomb formalism with a β line profile calculated from the full Coulomb impact formalism of Griem, Blaha, and Kepple.

$Ly - \beta$, Ar^{+17}

$T = 800.0\ eV$

$n_e = 1.0 \times 10^{24}/cc$

—— Full Coulomb Calculation

--- Kepple

Figure 7   Comparison of an Argon Lyman β line profile calculated from this full Coulomb formalism at a plasma density of 8.2×10^{23} electrons/cm^3 and a temperature of 800 eV (light line) with a β line profile calculated from the full Coulomb impact formalism of Griem, Blaha, and Kepple at 10^{24} electrons/cm^3 and 800 eV (dark line).
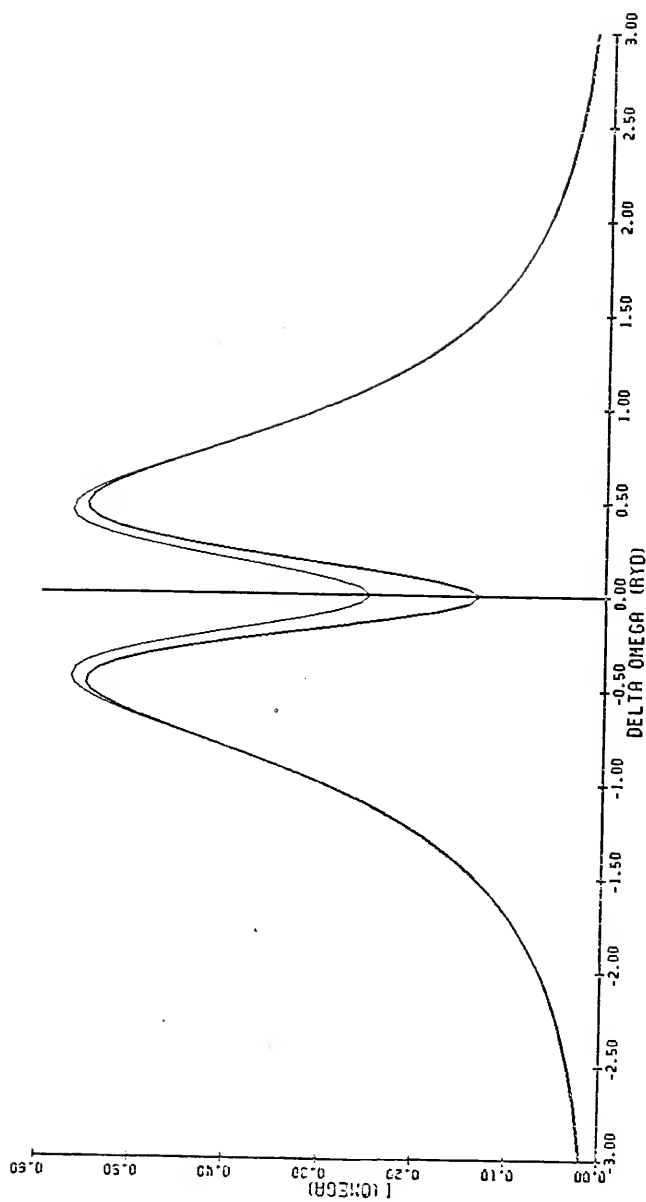
Line Shifts

Our objective here is to examine the line asymmetry which is caused by the static and dynamic shifts, B and $M_R(\Delta\omega)$, and to determine the significance of the dynamic shift in comparison to the static shift. We obtain $M_R(\Delta\omega)$ by the numerical evaluation of Eqs. (2.14) and (2.15). Several calculations of static shifts due to mean field effects of the plasma on the radiator have been done (Skupsky 1980; Davis and Blaha 1981; and references cited therein). Although some uncertainties remain in these calculations, for our purposes we will use the results of Skupsky (1980, 1982) for the static shift. These results were obtained by the numerical solution of the Schrödinger equation for a hydrogenic ion in a self consistent potential determined by the nonlinear Poisson equation for electrons and neighboring ions.

The Lyman β lines in Figure 8 include the static shift (solid line) and the static plus the dynamic shift (dashed line). The static shift causes an asymmetry, the lower energy (red) wing having the greater intensity. The dynamic shift causes a slight red shift of the line but has no significant effect on its shape. This full Coulomb result for the dynamic shift is significantly smaller than that obtained in the dipole approximation (Woltz et al. 1982).

Interaction Matrix Elements

In Figure 9 we compare Lyman β lines calculated with (solid line) and without (dashed line) radiator–perturbing ion and radiator–perturbing electron interaction matrix elements between states of principal quantum number 3 and 4 (see Section II.4). The inclusion of these matrix elements causes the line to be asymmetric, with the blue

Figure 8   Argon Lyman β line profiles including the static shift (solid line) and the static plus dynamic shift (dashed line). Density = 10^{24} electrons/cm^3, temperature = 800 eV.
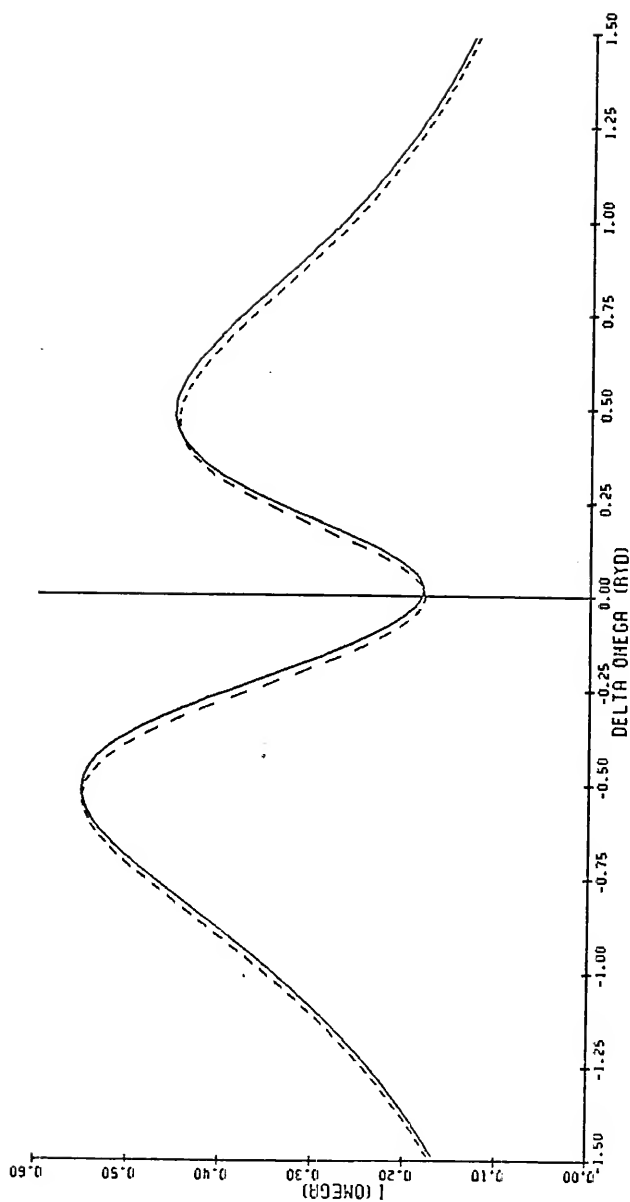
Figure 9   Comparison of Argon Lyman β line profiles calculated with (solid line) and without (dashed line) radiator-perturbing ion and radiator-perturbing electron interaction matrix elements between radiator states of principal quantum number 3 and 4. Density = 10^{24} electrons/cm^3, temperature = 800 eV.
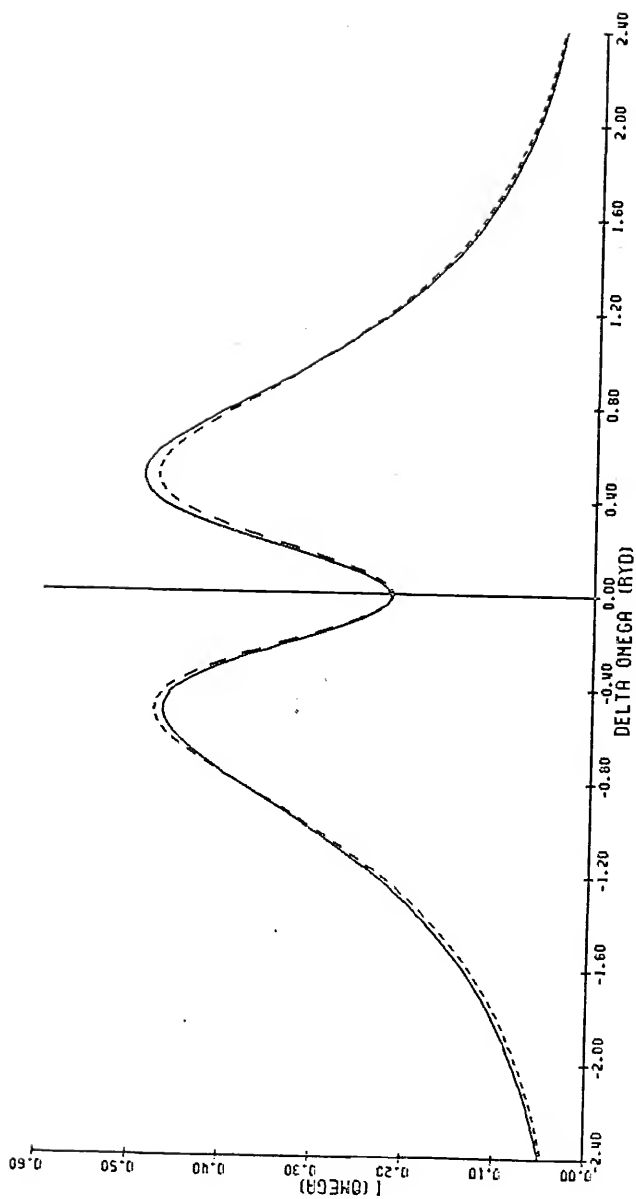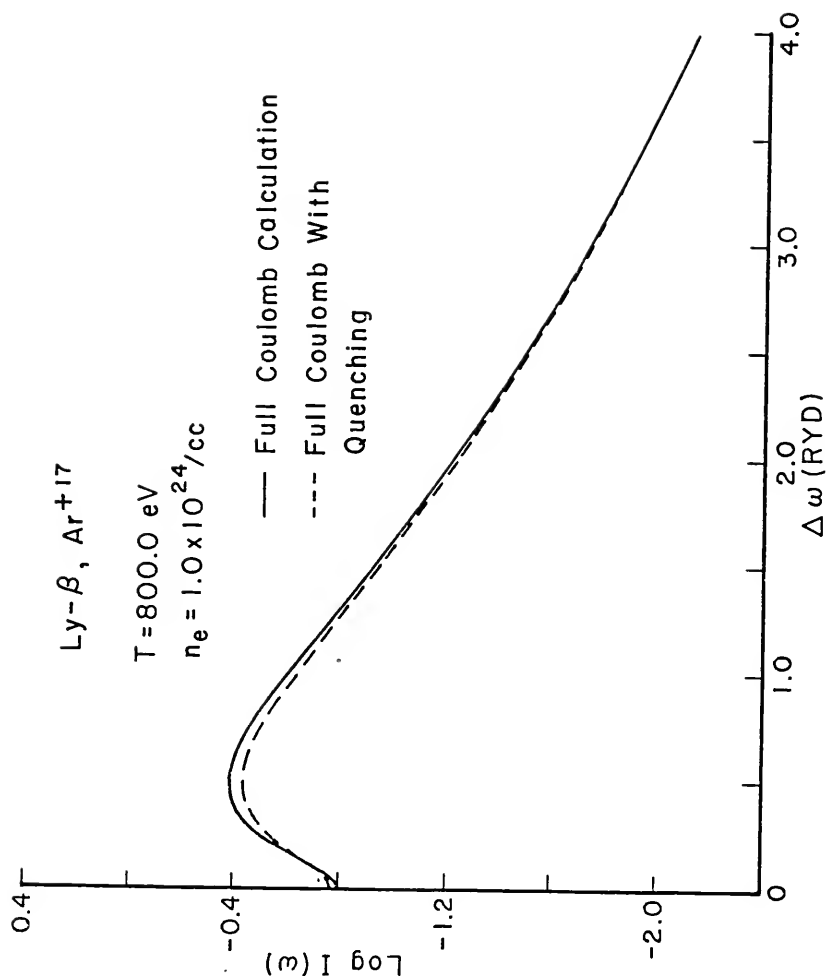
Figure 10   Comparison of Argon Lyman β line profiles calculated with (solid line) and without (dashed line) radiator-perturbing electron interaction matrix elements between radiator states of principal quantum number 3 and 4. Density = 10^{24} electrons/cm^3, temperature = 800 eV.

Ly-β, Ar^{+17}

T=800.0 eV
n_e=1.0 x 10^{24}/cc

—— Full Coulomb Calculation

--- Full Coulomb With
      Quenching

$\Delta \omega$(RYD)

Log I (ω)

peak more intense than the red peak and the red wing more intense than
the blue wing. To distinguish between ion and electron effects, we set
the ion perturbation matrix elements equal to zero while retaining the
electron perturbation matrix elements, obtaining the solid line in
Figure 10. This line is symmetric, and it is slightly broader due to
quenching than the dashed line, in which quenching has been neglected.
The asymmetry of the β line in Figure 9 is primarily due to quadratic
Stark shifting of radiator energy levels by the ion microfield. To show
this, we have included the quadratic Stark effect in an otherwise
symmetric Lyman β line calculation by adding the quadratic shift (Bethe
and Salpeter 1977),

$$\Delta E = - \frac{1}{16} a_o^2 \left(\frac{n}{Z_r}\right)^4 \epsilon^2 \left[17n^2 - 3q^2 - 9m^2 + 19\right]$$

to the diagonal elements of the matrix

$$\langle 3qm | \Delta\omega - M_I(\Delta\omega) | 3q'm' \rangle$$

(see Eq. 1.5.19). Here the kets $|nqm\rangle$ represent states of the radiator
calculated in parabolic coordinates, and the quantum number q is equal
to the difference of the quantum numbers n_1 and n_2 used by Bethe and
Salpeter. This calculation gives a Lyman β line which has an asymmetry
nearly identical to that of the β line in Figure 9, with the only
noticeable difference being that this calculation gives a slightly
larger peak asymmetry. The calculation of Figure 9 does not give the
exact quadratic Stark effect since it does not include radiator-ion
perturbation matrix elements between radiator states of all principal

quantum numbers, but the near agreement of these two calculations shows that the matrix elements between states of n=3 and 4 are responsible for a major part of the quadratic Stark shift. The asymmetry of Figure 9 is similar to the asymmetry obtained by Griem (1954) from a Hydrogen Balmer β line calculation which included the quadratic Stark effect.

CHAPTER IV
CONCLUSION

In this work we have extended the line shape formalism of Tighe
(1977) and Tighe and Hooper (1976, 1978) by eliminating the dipole
approximation which they used for the radiator-perturbing electron
interaction, retaining instead the full Coulomb radiator-perturbing
electron interaction. We calculate the line width and shift operator,
$M(\omega)$, to second order in this interaction. A second order calculation
of $M(\omega)$ will give good results for the part of the line profiles in
which we are interested, i.e. separations from line center less than or
on the order of the electron plasma frequency, since the electron
broadening of this part of the line is primarily due to weak electron-
radiator collisions. Our full Coulomb calculation gives Lyman α and β
lines which are only slightly broader than those calculated from the
dipole approximation, but the near agreement of the two calculations is
partly fortuitous. In the dipole approximation, broadening due to the
other multipoles of the interaction is neglected, but this is partially
compensated by the fact that the dipole approximation overestimates the
dipole part of the Coulomb interaction for perturbers which are less
than a few times the average radiator diameter from the radiator.

The Lyman α and β line profiles which we have obtained from this
full Coulomb calculation are somewhat broader than corresponding line
profiles calculated by Griem et al. (1979) from a classical path impact
theory with quantum mechanical corrections for strong collisions between

56

the radiator and perturbing electrons. For plasma conditions on the order of 10^{24} electrons/cm^3 and 800 eV, density diagnostics based on our Lyman β line would indicate a plasma density about 18% lower than would those based on the β line of Griem et al.

We have calculated the dynamic line shift due to perturbing electrons, obtaining a small red shift of about 0.03 Ryd. for a Lyman β line calculated for the plasma conditions of 10^{24} electrons/cm^3 and 800 eV. This shift is significantly smaller than that obtained in a similar calculation in which the dipole approximation for the radiator-perturbing electron interaction was used. The effect of the dynamic shift calculated here is considerably smaller than that of the static shift (Skupsky 1980, 1982), which causes an asymmetry in the β line, with the red wing having the greater intensity. This asymmetry results from different static shifts of the various angular momentum states which contribute to the line.

We have included in the calculation of a Lyman β line the ion-radiator and electron-radiator perturbation matrix elements between the initial states of the radiator, principal quantum number = 3, and the nearest adjacent energy level, principal quantum number = 4. The inclusion of these matrix elements gives an asymmetric line, with the blue peak more intense than the red peak and the red wing more intense than the blue wing. The asymmetry is due to the matrix elements of the ion-radiator perturbation, which cause nonlinear Stark shifts of the radiator energy levels. The electron-radiator perturbation causes a slight additional broadening of the line due to quenching.

Sholin (1969) has shown that when the quadratic Stark effect causes a significant line asymmetry, the quadrupole interaction between the

radiator and the ions will also have a significant effect on the line profile. Calculations of Balmer and Paschen β lines which include the quadrupole interaction (Pittman and Kelleher 1981) give asymmetric line profiles with the blue peak being more intense than the red peak. The quadrupole interaction should cause a similar asymmetry in the Lyman β line, although the magnitude of the asymmetry for the spectral lines and plasma conditions of interest here remains to be determined. This and the quadratic Stark effect may be significant causes of increased intensity of the blue peak of Argon Lyman β, an asymmetry which has been inferred from some recent laser implosion experiments (Yaakobi 1982).

APPENDIX A

MATRIX ELEMENTS OF M(ω)

Here we will use the No-Quenching Approximation (NQA) and the No Lower State Broadening Approximation (NLBA) to write M(ω) (Eq. 1.6.4) in the matrix form given by Eq. (1.6.7).

We see from Eq. (1.5.19) that since M(ω) appears in the inverse operator $[\omega-L(r)-B-M(\omega)]^{-1}$, which can be considered as a power series expansion, it acts on

$$[L(r)+B+M(\omega)]^k f(r)\vec{d}, \; k \geqslant 0 \; .$$

Here, the operator f(r) weights initial radiator states and the operator $\vec{d}$ determines transition probabilities between initial and final radiator states; so the only matrix elements of $f(r)\vec{d}$ which contribute significantly to a given line are of the type $[f(r)\vec{d}]_{if}$, where i and f represent initial and final radiator states for that line (Griem 1974). We can set all other matrix elements of $f(r)\vec{d}$ equal to zero. Let us define the operator

$$\vec{D}^{(k)} = [L(r)+B+M(\omega)]^k f(r)\vec{d} . \tag{A1}$$

All matrix elements of $\vec{D}^{(0)}$ which are not of the form $\vec{D}^{(0)}_{if}$ are set equal to zero. We will show that as a consequence of this matrix structure of $\vec{D}^{(0)}$, the matrix elements of $M(\omega)\vec{D}^{(0)}$, when restricted by the NQA and

59

the NLBA, can be written as (Smith 1966)

$$[M(\omega)\vec{D}^{(0)}]_{if} = \sum_{i'} M(\omega)_{ii'} \; \vec{D}^{(0)}_{i'f} \; , \tag{A2}$$

where $M(\omega)_{ii'}$ is given by Eq. (1.6.7). Next we will show that $\vec{D}^{(k)}$ has the same matrix structure as $\vec{D}^{(0)}$, so Eq. (A2) holds for all $\vec{D}^{(k)}$ and the matrix form of $M(\omega)$ (Eq. 1.6.7) can be used to calculate $[\omega - L(r) - B - M(\omega)]^{-1}$.

If we let μ and ν represent arbitrary radiator states, the matrix elements of $M(\omega)\vec{D}^{(0)}$, where $M(\omega)$ is given by Eq. (1.6.4), can be written as

$$
\begin{aligned}
[M(\omega)\vec{D}^{(0)}]_{\mu\nu} = &-\frac{in}{\hbar^2} \mathrm{Tr}_1 \int_0^\infty dt \; e^{i\omega t} \\
&\times \Big[\sum_{\mu'if} V_{\mu\mu'} \, e^{-i(E_\mu + H(1))t/\hbar} \; V_{\mu'i} f(1)\vec{D}^{(0)}_{if} \, e^{i(E_f + H(1))t/\hbar} \; \delta_{f\nu} \\
&- \sum_{if} V_{\mu i} e^{-i(E_i + H(1))t/\hbar} \, f(1)\vec{D}^{(0)}_{if} \, V_{f\nu} \, e^{i(E_\nu + H(1))t/\hbar} \\
&- \sum_{if} e^{-i(E_\mu + H(1))t/\hbar} \, V_{\mu i} f(1)\vec{D}^{(0)}_{if} \, e^{i(E_f + H(1))t/\hbar} \; V_{f\nu} \\
&+ \sum_{if\nu'} \delta_{\mu i} \, e^{-i(E_i + H(1))t/\hbar} \, f(1)\vec{D}^{(0)}_{if} V_{f\nu'} e^{i(E_{\nu'} + H(1))t/\hbar} \; V_{\nu'\nu} \Big] \; , \tag{A3}
\end{aligned}
$$

where we have written the term $[\omega - L(r) - L(1)]^{-1}$ in $M(\omega)$ as a time transform and we have replaced the Liouville operators by the corresponding commutators. Here, $V_{\mu\mu'}$ represents matrix elements of $V_1(r,1)$.

Now we use the NQA and the NLBA to simplify this expression. In the NQA, we assume that the perturbing electrons do not cause the

radiator to make nonradiative transitions between states of different
principal quantum number; that is, the matrix elements $V_{\mu\mu'}$ are nonzero
only if the states μ and μ' have the same principal quantum number.
This restricts the μ's to be initial states and the ν's to be final
states in Eq. (A3). We will examine the significance of quenching in
Section 2.4. In the NLBA, we assume that there is no broadening of the
final radiator state by the perturbing electrons, so we set the matrix
elements $V_{ff'}$ equal to zero. This is a good approximation for Lyman
lines since the final (ground) state and the plasma have no dipole
interaction, which is the most significant multipole in broadening.
With these approximations, the second, third, and fourth terms in brack-
ets in Eq. (A3) are equal to zero, and the first term can be written as

$$\left[M(\omega)\vec{D}^{(0)} \right]_{if} =$$

$$- \frac{in}{\hbar^2} \mathrm{Tr}_1 \int_0^\infty dt \sum_{i'i''} e^{i\Delta\omega t} V_{ii''} e^{-iH(1)t/\hbar} V_{i''i',f(1)} \vec{D}^{(0)}_{i'f} e^{iH(1)t/\hbar} \tag{A4}$$

where

$$\Delta\omega = \omega - (E_{i''} - E_f)/\hbar \ .$$

If the final states are degenerate, Eq. (A4) can be written as the
matrix product

$$\left[M(\omega)\vec{D}^{(0)} \right]_{if} = \sum_{i'} M(\omega)_{ii'} \vec{D}^{(0)}_{i'f}$$

where

$$M(\omega)_{ii'} = -\frac{in}{\hbar^2} \, \mathrm{Tr}_1 \int_0^\infty dt \sum_{i''} e^{i\Delta\omega t} V_{ii''} e^{-iH(1)t/\hbar} V_{i''i'} e^{iH(1)t/\hbar} f(1) .$$

(A5)

We must have degenerate final states (or, as in the case of Lyman lines, one final state) to go from Eq. (A4) to Eq. (A5) since the $\Delta\omega$ in $M(\omega)_{ii'}$ contains E_f.

We see from Eq. (A4) that the only nonzero matrix elements of $M(\omega)\vec{D}^{(0)}$ are $\left[M(\omega)\vec{D}^{(0)}\right]_{if}$. This is a consequence of the NQA, the NLBA, and the fact that the only nonzero matrix elements of $\vec{D}^{(0)}$ are $\vec{D}^{(0)}_{if}$. Similarly, it can be shown that the only nonzero matrix elements of $[L(r) + B]\vec{D}^{(0)}$ are $\left\{[L(r) + B]\vec{D}^{(0)}\right\}_{if}$, so $\vec{D}^{(1)}$ only has nonzero elements $\vec{D}^{(1)}_{if}$. By induction, the only nonzero elements of $\vec{D}^{(k)}$ for all $k > 0$ are $\vec{D}^{(k)}_{if}$; so Eq. (A4) holds for $\vec{D}^{(k)}$ as well as $\vec{D}^{(0)}$. Hence, we can use Eq. (A5) to calculate $M(\omega)$ in $[\omega - L(r) - B - M(\omega)]^{-1}$.

APPENDIX B

EVALUATION OF $G(k_1, k_2)$

In this appendix we reduce the function $G_{n\ell_1 m_1, n\ell_2 m_2}(k_1, k_2)$ (Eq. 2.1.7) to a form which is tractable for numerical calculation. We have

$$
G_{n\ell_1 m_1, n\ell_2 m_2}(k_1, k_2) = n_e \lambda_T^3 k_1^2 k_2^2 \sum_{\ell_3 m_3} \sum_{\ell_4 m_4} \sum_{\ell_6 m_6}
$$

$$
\times \langle k_1 \ell_4 m_4 n \ell_1 m_1 | V_1(r,1) | k_2 \ell_6 m_6 n \ell_3 m_3 \rangle \langle k_2 \ell_6 m_6 n \ell_3 m_3 | V_1(r,1) | k_1 \ell_4 m_4 n \ell_2 m_2 \rangle \ .
$$

$$(B1)$$

The expression for $V_1(r,1)$, Eq. (1.6.3), can be expanded in spherical harmonics (Jackson 1975) to obtain

$$
V_1(r,1) = \frac{e^2}{|\vec{x} - \vec{x}_r|} - \frac{e^2}{|\vec{x}|}
$$

$$
= 4\pi e^2 \sum_{\ell=0}^{\infty} \sum_{m=-\ell}^{\ell} \frac{1}{(2\ell+1)} \left(\frac{x_<^{\ell_5}}{x_>^{\ell_5+1}} - \frac{\delta_{\ell_5,0}}{x} \right) Y_{\ell m}^*(\hat{x}) Y_{\ell m}(\hat{x}_r) \ ,
$$

$$(B2)$$

where $\vec{x}$ and $\vec{x}_r$ are the positions of the perturbing electron and the radiator electron, and $x_<$ ($x_>$) refers to the lesser (greater) of x and x_r. With this expansion and the expression for the perturber wavefunctions, Eq. (2.1.1), the first matrix element of $V_1(r,1)$ in Eq. (B1) can be written as

$$
\langle k_1 \ell_4 m_4 n \ell_1 m_1 | V_1(r,1) | k_2 \ell_6 m_6 n \ell_3 m_3 \rangle =
$$

63

$$8e^2 \, i^{\ell_6 - \ell_4} \, e^{i\left(\sigma(\ell_6, k_2) - \sigma(\ell_4, k_1)\right)} \sum_{\ell_5 m_5}^{64} \frac{1}{(2\ell_5 + 1)}$$

$$\times \left(\int d\hat{x} \, Y^*_{\ell_4 m_4}(\hat{x}) Y_{\ell_5 m_5}(\hat{x}) Y_{\ell_6 m_6}(\hat{x}) \right) \left(\int d\hat{x}_r Y^*_{\ell_1 m_1}(\hat{x}_r) Y_{\ell_5 m_5}(\hat{x}_r) Y_{\ell_3 m_3}(\hat{x}_r) \right)$$

$$\times \left(\int_0^\infty dx \, x^2 (k_1 x)^{-1} (k_2 x)^{-1} F_{\ell_4}(\eta_1, k_1 x) F_{\ell_6}(\eta_2, k_2 x) A_{\ell_1 \ell_3 \ell_5}(x) \right) \qquad \text{(B3)}$$

where

$$A_{\ell_1 \ell_3 \ell_5}(x) = \int_0^\infty dx_r \, x_r^2 R_{n\ell_1}(x_r) \left(\frac{x_<^{\ell_5}}{x_>^{\ell_5 + 1}} - \frac{\delta_{\ell_5, 0}}{x} \right) R_{n\ell_3}(x_r) , \qquad \text{(B4)}$$

and $R_{n\ell}(x_r)$ is the hydrogenic wavefunction of the radiator. In Appendix C we obtain a form of Eq. (B4) convenient for computation. The integral of three spherical harmonics is given by (Edmonds 1957)

$$\int d\hat{x} \, Y_{\ell_1 m_1}(\hat{x}) Y_{\ell_2 m_2}(\hat{x}) Y_{\ell_3 m_3}(\hat{x})$$

$$= \left[\frac{(2\ell_1 + 1)(2\ell_2 + 1)(2\ell_3 + 1)}{4\pi} \right]^{1/2} \begin{pmatrix} \ell_1 & \ell_2 & \ell_3 \\ m_1 & m_2 & m_3 \end{pmatrix} \begin{pmatrix} \ell_1 & \ell_2 & \ell_3 \\ 0 & 0 & 0 \end{pmatrix} \qquad \text{(B5)}$$

where

$$\begin{pmatrix} \ell_1 & \ell_2 & \ell_3 \\ m_1 & m_2 & m_3 \end{pmatrix}$$

is the Wigner 3-j symbol. We use this equation and the fact that

$$Y^*_{\ell m}(\hat{x}) = (-1)^m Y_{\ell -m}(\hat{x})$$

to obtain

$$\langle k_1 \ell_4 m_4 n \ell_1 m_1 | V_1(r, 1) | k_2 \ell_6 m_6 n \ell_3 m_3 \rangle = \frac{2e^2}{\pi k_1 k_2} \, i^{\ell_6 - \ell_4} \, e^{i\left(\sigma(\ell_6, k_2) - \sigma(\ell_4, k_1)\right)}$$

$$\times \sum_{\ell_5 m_5} (-1)^{m_1+m_4+m_5} [(2\ell_1+1)(2\ell_3+1)(2\ell_4+1)(2\ell_6+1)]^{1/2}$$

$$\times \begin{pmatrix} \ell_1 & \ell_3 & \ell_5 \\ -m_1 & m_3 & m_5 \end{pmatrix} \begin{pmatrix} \ell_4 & \ell_5 & \ell_6 \\ -m_4 & -m_4 & m_6 \end{pmatrix} \begin{pmatrix} \ell_1 & \ell_3 & \ell_5 \\ 0 & 0 & 0 \end{pmatrix} \begin{pmatrix} \ell_4 & \ell_5 & \ell_6 \\ 0 & 0 & 0 \end{pmatrix}$$

$$\times \int_o^\infty dx \, F_{\ell_4}(\eta_1, k_1 x) F_{\ell_6}(\eta_2, k_2 x) A_{\ell_1 \ell_3 \ell_5}(x). \qquad (B6)$$

Similarly, we obtain for the second matrix element of $V_1(r,1)$ appearing in Eq. (B1):

$$\langle k_2 \ell_6 m_6 n \ell_3 m_3 | V_1(r,1) | k_1 \ell_4 m_4 n \ell_2 m_2 \rangle = \frac{2e^2}{\pi k_1 k_2} i^{\ell_4 - \ell_6} e^{i(\sigma(\ell_4,k_1) - \sigma(\ell_6,k_2))}$$

$$\times \sum_{\ell_7 m_7} (-1)^{m_3+m_6+m_7} [(2\ell_3+1)(2\ell_2+1)(2\ell_6+1)(2\ell_4+1)]^{1/2}$$

$$\times \begin{pmatrix} \ell_3 & \ell_2 & \ell_7 \\ -m_3 & m_2 & m_7 \end{pmatrix} \begin{pmatrix} \ell_6 & \ell_7 & \ell_4 \\ -m_6 & -m_7 & m_4 \end{pmatrix} \begin{pmatrix} \ell_3 & \ell_2 & \ell_7 \\ 0 & 0 & 0 \end{pmatrix} \begin{pmatrix} \ell_6 & \ell_7 & \ell_4 \\ 0 & 0 & 0 \end{pmatrix}$$

$$\times \int_o^\infty dx \, F_{\ell_6}(\eta_2, k_2 x) F_{\ell_4}(\eta_1, k_1 x) A_{\ell_3 \ell_2 \ell_7}(x). \qquad (B7)$$

We use Eqs. (B6) and (B7) to write Eq. (B1) as

$$G_{n\ell_1 m_1, n\ell_2 m_2}(k_1, k_2) =$$

$$\frac{4n_e \lambda_T^3 e^4}{\pi^2} \sum_{\ell_3 \ell_4 \ell_6} \sum_{\ell_5 \ell_7} [(2\ell_1+1)(2\ell_2+1)]^{1/2}(2\ell_3+1)(2\ell_4+1)(2\ell_6+1)$$

$$\times \left(\int_o^\infty dx \, F_{\ell_4}(\eta_1, k_1 x) F_{\ell_6}(\eta_2, k_2 x) A_{\ell_1 \ell_3 \ell_5}(x) \right)$$

$$\times \left(\int_o^\infty dx \, F_{\ell_6}(\eta_2, k_2 x) F_{\ell_4}(\eta_1, k_1 x) A_{\ell_3 \ell_2 \ell_7}(x) \right)$$

$$\times \begin{pmatrix} \ell_1 & \ell_3 & \ell_5 \\ 0 & 0 & 0 \end{pmatrix} \begin{pmatrix} \ell_4 & \ell_5 & \ell_6 \\ 0 & 0 & 0 \end{pmatrix} \begin{pmatrix} \ell_2 & \ell_3 & \ell_7 \\ 0 & 0 & 0 \end{pmatrix} \begin{pmatrix} \ell_4 & \ell_6 & \ell_7 \\ 0 & 0 & 0 \end{pmatrix}$$

$$\times \sum_{m_3 m_4 m_6} \sum_{m_5 m_7} (-1)^{m_1 + m_3 + m_4 + m_6 + m_5 + m_7}$$

$$\times \begin{pmatrix} \ell_2 & \ell_3 & \ell_5 \\ -m_1 & m_3 & m_5 \end{pmatrix} \begin{pmatrix} \ell_4 & \ell_6 & \ell_6 \\ -m_4 & -m_5 & m_6 \end{pmatrix} \begin{pmatrix} \ell_3 & \ell_2 & \ell_7 \\ -m_3 & m_2 & m_7 \end{pmatrix} \begin{pmatrix} \ell_6 & \ell_7 & \ell_4 \\ -m_6 & -m_7 & m_4 \end{pmatrix}. \tag{B8}$$

The m-sums in this equation can be done with the aid of the following properties of the 3-j symbols (Edmonds 1957):

(1) ℓ_1, ℓ_2 and ℓ_3 must satisfy the triangle inequality, $|\ell_1 - \ell_2| \leqslant \ell_3 \leqslant (\ell_1 + \ell_2)$, and $m_1 + m_2 + m_3$ must equal zero in order for the 3-j symbol

$$\begin{pmatrix} \ell_1 & \ell_2 & \ell_3 \\ m_1 & m_2 & m_3 \end{pmatrix}$$

to be nonzero.

(2) The completeness relation:

$$\sum_{m_1 m_2} \begin{pmatrix} \ell_1 & \ell_2 & \ell_3 \\ m_1 & m_2 & m_3 \end{pmatrix} \begin{pmatrix} \ell_1 & \ell_2 & \ell_3' \\ m_1 & m_2 & m_3' \end{pmatrix} = (2\ell_3 + 1)^{-1} \delta_{\ell_3 \ell_3'} \delta_{m_3 m_3'} \Delta(\ell_1, \ell_2, \ell_3) \ ,$$

where $\Delta(\ell_1, \ell_2, \ell_3)$ is one if ℓ_1, ℓ_2, ℓ_3 satisfy the triangle inequality and zero if they do not.

(3) An odd permutation of the columns of a 3-j symbol is equivalent to multiplication by $(-1)^{\ell_1 + \ell_2 + \ell_3}$:

$$\begin{pmatrix} \ell_1 & \ell_2 & \ell_3 \\ m_1 & m_2 & m_3 \end{pmatrix} = (-1)^{\ell_1 + \ell_2 + \ell_3} \begin{pmatrix} \ell_2 & \ell_1 & \ell_3 \\ m_2 & m_1 & m_3 \end{pmatrix} \ .$$

(4)   Changing the sign of all the m's is equivalent to multiplication by $(-1)^{\ell_1 + \ell_2 + \ell_3}$:

$$\begin{pmatrix} \ell_1 & \ell_2 & \ell_3 \\ m_1 & m_2 & m_3 \end{pmatrix} = (-1)^{\ell_1 + \ell_2 + \ell_3} \begin{pmatrix} \ell_1 & \ell_2 & \ell_3 \\ -m_1 & -m_2 & -m_3 \end{pmatrix} \ .$$

A special case of this rule is that if $m_1 = m_2 = m_3 = 0$, $\ell_1 + \ell_2 + \ell_3$ must be even or the 3-j sumbol will be equal to zero.

First we do the m_4 and m_6 sums,

$$\sum_{m_4 m_6} (-1)^{m_4 + m_6} \begin{pmatrix} \ell_4 & \ell_5 & \ell_6 \\ -m_4 & -m_5 & m_6 \end{pmatrix} \begin{pmatrix} \ell_6 & \ell_7 & \ell_4 \\ -m_6 & -m_7 & m_4 \end{pmatrix} = (-1)^{m_5} \sum \begin{pmatrix} \ell_4 & \ell_6 & \ell_5 \\ m_4 & m_6 & m_5 \end{pmatrix} \begin{pmatrix} \ell_4 & \ell_6 & \ell_7 \\ m_4 & -m_6 & -m_7 \end{pmatrix}$$

$$= (-1)^{m_5} (2\ell_5 + 1) \delta_{\ell_5 \ell_7} \delta_{m_5, -m_7} \Delta(\ell_4, \ell_6, \ell_5) \ . \tag{B9}$$

Next we use the Kronecker delta in m_5 and $-m_7$ to do the sum over m_7, then the m_3 and m_5 sums are

$$\sum_{m_3 m_5} (-1)^{m_3 + m_5} \begin{pmatrix} \ell_1 & \ell_3 & \ell_5 \\ -m_1 & m_3 & m_5 \end{pmatrix} \begin{pmatrix} \ell_2 & \ell_3 & \ell_5 \\ m_2 & -m_3 & -m_5 \end{pmatrix}$$

$$= (-1)^{m_1} (-1)^{\ell_1 + \ell_3 + \ell_5} \sum_{m_3 + m_5} \begin{pmatrix} \ell_1 & \ell_3 & \ell_5 \\ m_1 & -m_3 & -m_5 \end{pmatrix} \begin{pmatrix} \ell_2 & \ell_3 & \ell_5 \\ m_2 & -m_3 & -m_5 \end{pmatrix}$$

$$= (-1)^{m_1 + \ell_1 + \ell_3 + \ell_5} (2\ell_1 + 1)^{-1} \delta_{\ell_1 \ell_2} \delta_{m_1 m_2} \Delta(\ell_1, \ell_3, \ell_5) \ . \tag{B10}$$

Using these results, we write Eq. (B8) as

$$G_{n\ell_1 m_1, n\ell_2 m_2}(k_1, k_2) = \frac{4 n_e \lambda_T^3 e^4}{\pi^2} \delta_{\ell_1 \ell_2} \delta_{m_1 m_2}$$

$$\times \sum_{\ell_3=0}^{n-1} \sum_{\ell_5=0}^{2n-2} \sum_{\ell_4, \ell_6=0}^{\infty} \frac{(2\ell_3+1)(2\ell_4+1)(2\ell_6+1)}{(2\ell_5+1)} \begin{pmatrix} \ell_1 & \ell_3 & \ell_5 \\ 0 & 0 & 0 \end{pmatrix} \begin{pmatrix} \ell_4 & \ell_5 & \ell_6 \\ 0 & 0 & 0 \end{pmatrix}^2$$

$$\times \left[\int_0^{\infty} dx \, F_{\ell_4}(\eta_1, k_1 x) F_{\ell_6}(\eta_2, k_2 x) A_{\ell_1 \ell_3 \ell_5}(x) \right]^2 . \tag{B11}$$

This is the desired result, Eq. (2.1.8). We use this equation (with Eq. (C.8) for A(x)) to calculate $G(k_1, k_2)$ numerically, then the results for $G(k_1, k_2)$ are used in Eqs. (2.1.12)-(2.1.15) to obtain $M(\omega)$.

A COMPUTATIONAL FORM FOR $A_{\ell_1\ell_2\ell_3}(x)$

Here we reduce the term $A_{\ell_1\ell_2\ell_3}(x)$ to a form which is practical for computer evaluation. We start with Eq. (2.1.9),

$$A_{\ell_1\ell_2\ell_3}(x) = \int_0^\infty dx_r x_r^2 \, R_{n\ell_1}(x_r)\left(\frac{x_<^{\ell_3}}{x_>^{\ell_3+1}} - \frac{\delta_{\ell_3,0}}{x}\right) R_{n\ell_2}(x_r), \qquad (C1)$$

where $x_<$ $(x_>)$ is the lesser (greater) of x and x_r, which are the radial coordinates of the perturber and radiator, respectively. The function $R_{n\ell}(x_r)$ is the hydrogenic radial wavefunction for a radiator with nuclear charge Z (Messiah 1961),

$$R_{n\ell}(x_r) = \left\{\frac{(n-\ell-1)!}{2n[(n+\ell)!]^3}\right\}^{1/2} e^{-x_r/2} \, x_r^\ell \, L_{n-\ell-1}^{2\ell+1}(x_r), \qquad (C2)$$

where x and x_r have been scaled in terms of $\frac{na_o}{2Z}$, and L is the Laguerre polynomial,

$$L_{n-\ell-1}^{2\ell+1}(x) = \sum_{k=0}^{n-\ell-1} (-1)^k \frac{[(n+\ell)!]^3 x^k}{(n-\ell-1-k)!(2\ell+1+k)!k!} \cdot \qquad (C3)$$

If we substitute Eqs. (C2) and (C3) into Eq. (C1) we obtain

$$A_{\ell_1\ell_2\ell_3}(x) =$$

$$\sum_{k_1=0}^{n-\ell_1-1} \sum_{k_2=0}^{n-\ell_2-1} C_{k_1k_2} \int_0^\infty dx_r x_r^{k_1+k_2+\ell_1+\ell_2+2} \, e^{-x_r}\left(\frac{x_<^{\ell_3}}{x_>^{\ell_3+1}} - \frac{\delta_{\ell_3,0}}{x}\right) \qquad (C4)$$

where

$$C_{k_1 k_2} =$$

$$(-1)^{k_1+k_2} \frac{[(n-\ell_1-1)!(n-\ell_2-1)!(n+\ell_1)!(n+\ell_2)!}{2n(n-\ell_1-k_1-1)!(n-\ell_2-k_2-1)!(2\ell_1+1+k_1)!(2\ell_2+1+k_2)!k_1!k_2!} \quad . \quad (C5)$$

We see from Eq. (2.1.8) that $A_{\ell_1 \ell_2 \ell_3}(x)$ will be multiplied by a 3-j symbol containing ℓ_1, ℓ_2, and ℓ_3, so ℓ_1, ℓ_2, and ℓ_3 must satisfy the triangle inequality, $|\ell_1-\ell_2| < \ell_3 < (\ell_1+\ell_2)$. Also, k_1 and k_2 are greater than or equal to zero. Therefore the exponent of x_r in Eq. (C4) is always positive, and we can use the definite integrals

$$\int_o^x dx_r \, x_r^m \, e^{-x_r} = m!(1 - e^{-x} \sum_{j=0}^m \frac{x^j}{j!}), \quad m > 0 , \quad (C6)$$

and

$$\int_x^\infty dx_r \, x_r^m \, e^{-x_r} = m! \, e^{-x} \sum_{j=0}^m \frac{x^j}{j!} , \quad m > 0 , \quad (C7)$$

to write Eq. (C4) as

$$A_{\ell_1 \ell_2 \ell_3}(x) = \sum_{k_1=0}^{n-\ell_1-1} \sum_{k_2=0}^{n-\ell_2-1} C_{k_1 k_2}$$

$$\times \left[\frac{(1-\delta_{\ell_3,0})}{x^{\ell_3+1}} (k_1+k_2+\ell_1+\ell_2+\ell_3+2)!(1 - e^{-x} \sum_{j=0}^{(k_1+k_2+\ell_1+\ell_2+\ell_3+2)} \frac{x^j}{j!}) \right.$$

$$+ x^{\ell_3}(k_1+k_2+\ell_1+\ell_2-\ell_3+1)! \, e^{-x} \sum_{j=0}^{(k_1+k_2+\ell_1+\ell_2-\ell_3+1)} \frac{x^j}{j!}$$

$$\left. - \frac{\delta_{\ell_3,0}}{x} (k_1+k_2+\ell_1+\ell_2+2)! \, e^{-x} \sum_{j=0}^{(k_1+k_2+\ell_1+\ell_2+2)} \frac{x^j}{j!} \right] . \quad (C8)$$

This equation is used in the numerical calculation of $A_{\ell_1 \ell_2 \ell_3}(x)$.

APPENDIX D
NUMERICAL METHODS

To obtain numerical results for the line profiles, we calculate $M_I(\Delta\omega)$ and $M_R(\Delta\omega)$ numerically, then use these results in a line shape program by Tighe (1977). This program calculates $J(\omega,\varepsilon)$ by inverting the matrix

$$\left[\Delta\omega - \left(H(r)/\hbar - \omega_1\right) - B - M(\omega)\right]$$

(Eq. 1.5.19), then does the ion microfield integration (Eq. 1.4.13) to obtain $I(\omega)$.

We calculate $M_I(\Delta\omega)$ from Eqs. (2.1.12) and (2.1.13), using Eq. (2.1.8) for $G(k_1,k_2)$. The Coulomb wavefunctions, which appear in Eq. (2.1.8), are calculated by a continued fraction expansion and recursion relations (Barnett et al. 1974). For small values of the argument kx the Coulomb wavefunctions are calculated from a series expansion (Abramowitz and Stegun 1972). We then use a trapezoidal rule integration to do the x-integral in $G(k_1,k_2)$. The 3-j symbols in $G(k_1,k_2)$ are calculated by a Fortran function given by Vidal et al. (1970). We make the change of variables $\beta\hbar^2 k_1^2/2m = y$ to put the k_1-integral of Eq. (2.1.12) into a form which can be integrated by Gauss-Laguerre quadrature.

We calculate $M_R(\Delta\omega)$ from Eqs. (2.1.14) and (2.1.15). The k_1-integral is done by Gauss-Legendre quadrature for a mesh of k_2 values, then a Simpson's rule integration is used to do the k_2-integral.

71

REFERENCES

Abramowitz, M. and Stegun, I. A. 1972, Handbook of Mathematical
Functions (Dover, New York).

Alder, K., Bohr, A., Huus, T., Mottelson, B., and Winther, A. 1956, Rev.
Mod. Phys. 28, 432.

Apruzese, J. P., Kepple, P. C., Whitney, K. G., Davis, J., and Duston,
D. 1981, Phys. Rev. A24, 1001.

Baranger, M. 1962, Atomic and Molecular Processes, D. R. Bates, Ed.
(Academic Press, Inc., New York), Chapter 13.

Baranger, M. and Mozer, B. 1959, Phys. Rev. 115, 521.

Barnett, A. R., Feng, D. H., Steed, J. W., and Goldfarb, L. J. B. 1974,
Computer Physics Communications 8, 377.

Bethe, H. A. and Salpeter, E. E. 1977, Quantum Mechanics of One- and
Two-Electron Atoms (Plenum, New York).

Biedenharn, L. C. 1956, Phys. Rev. 102, 262.

Bogoliubov, N. N. 1962, Studies in Statistical Mechanics, J. de Boer and
G. E. Uhlenbeck, Eds. (North-Holland, Amsterdam), Vol. I.

Brout, R. and Caruthers, P. 1963, Lectures on the Many-Electron Problem
(Wiley, New York).

Cooper, J. 1966, Plasma Spectroscopy, Rep. Progr. Phys. 29, 35.

Davis, J. and Blaha, M. 1981, NRL Memorandum Report 4689.

Dufty, J. W. and Boercker, D. B. 1976, J. Quant. Spectr. Radiative
Transfer 16, 1065.

Edmonds, A. R. 1957, Angular Momentum In Quantum Mechanics (Princeton
University Press, Princeton, New Jersey).

Fetter, A. L. and Walecka, J. D. 1971, Quantum Theory of Many-Particle
Systems (McGraw-Hill, New York).

Greene, R. L. 1979, Phys. Rev. A19, 2002.

Griem, H. R. 1954, Z. Phys. 137, 280.

72

Griem, H. R. 1964, Plasma Spectroscopy (McGraw-Hill Book Company, New York).

Griem, H. R. 1974, Spectral Line Broadening by Plasmas (Academic, New York).

Griem, H. R., Blaha, M., and Kepple, P. C. 1979, Phys. Rev. A19, 2421.

Hooper, C. F. Jr. 1968, Phys Rev. 165, 215.

Hussey, T. W. 1974, Dissertation (University of Florida).

Hussey, T. W., Dufty, J. W., and Hooper, C. F. 1975, Phys. Rev. A12, 1084.

Hussey, T. W., Dufty, J. W., and Hooper, C. F. Jr. 1977, Phys. Rev. A16, 1248.

Iglesias, C. I. 1982, Phys. Rev. A25, 1632.

Jackson, J. D. 1975, Classical Electrodynamics (Wiley, New York).

Karzas, W. J. and Latter, R. 1961, Astrophys. J. Supp. 55, 167.

Kepple, P. C. 1980, Naval Research Laboratory, private communication.

Kilkenny, J. D., Lee, R. W., Key, M. H., and Lunney, J. G. 1980, Phys. Rev. A22, 2746.

Lee, R. W. 1979, Phys. Lett. 71A, 224.

Messiah, A. 1961, Quantum Mechanics (Wiley, New York).

Mozer, B. and Baranger, M. 1960, Phys. Rev. 118, 626.

O'Brien, J. T. 1970, Dissertation (University of Florida).

O'Brien, J. T. 1971, Astrophys. J. 170, 613.

O'Brien, J. T. and Hooper, C. F. Jr. 1974, J. Quant. Spectr. Radiative Transfer 14, 479.

Pittman, T. L. and Kelleher, D. E. 1981, Spectral Line Shapes, B. Wende, Ed. (Walter de Gruyter, New York).

Seidel, J. 1980, Z. Naturforsch. 35a, 679.

Sholin, G. V. 1969, Optics and Spectroscopy 26, 419.

Skupsky, S. 1980, Phys. Rev. A21, 1316.

Skupsky, S. 1982, University of Rochester, private communication.
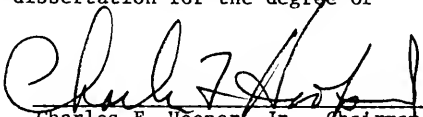
Smith, E. W. 1966, Dissertation (University of Florida).

Smith, E. W. 1968, Phys. Rev. 166, 102.

Smith, E. W., Cooper, J., Chappell, W. R., and Dillon, T. 1971a, J. Quant. Spectr. Radiative Transfer 11, 1547.

Smith, E. W., Cooper, J., Chappell, W. R., and Dillon, T. 1971b, J. Quant. Spectr. Radiative Transfer 11, 1567.

Smith, E. W., Cooper, J., and Vidal, C. R. 1969, Phys. Rev. 185, 140.

Smith, E. W., Cooper, J., and Vidal, C. R. 1970, J. Quant. Spectr. Radiative Transfer 10, 1011.

Smith, E. W. and Hooper, C. F. Jr. 1967, Phys. Rev. 157, 126.

Tighe, R. J. 1977, Dissertation (University of Florida).

Tighe, R. J. and Hooper, C. F. Jr. 1976, Phys. Rev. A14, 1514.

Tighe, R. J. and Hooper, C. F. Jr. 1977, Phys. Rev. A15, 1773.

Tighe, R. J. and Hooper, C. F. Jr. 1978, Phys. Rev. A17, 410.

Vidal, C. R., Cooper, J., and Smith, E. W. 1970, National Bureau of Standards Monograph 116 (Boulder, Colorado).

Woltz, L. A., Iglesias, C. A., and Hooper, C. F., Jr. 1982, J. Quant. Spectr. Radiative Transfer 27, 233.

Yaakobi, B. 1982, University of Rochester, private communication.

Yaakobi, B., Skupsky, S., McCrory, R. L., Hooper, C. F., Deckman, H., Bourke, P., and Soures, J. M. 1980, Phys. Rev. Lett. 44, 1072.

Yaakobi, B., Steel, D., Thorsos, E., Hauer, A., Perry, B. 1977, Phys. Rev. Lett. 39, 1526.

Yaakobi, B., Steel, D., Thorsos, E., Hauer, A., Perry, B., Skupsky, S., Geiger, J., Lee, C. M., Letzring, S., Rizzo, J., Mukaiyama, T., Lazarus, E., Halpern, G., Deckman, H., Delettrez, J., Soures, J., and McCrory, R. 1979, Phys. Rev. A19, 1247.

BIOGRAPHICAL SKETCH

Lawrence A. Woltz was born on August 29, 1949, in New Brunswick, New Jersey. He graduated from Southeast High School, Bradenton, Florida, in June 1967. He attended Manatee Junior College, then the University of South Florida, where he received the degree of Bachelor of Arts in physics in June 1971. He was a graduate student at the University of South Florida from September 1972 until August 1974. From September 1974 until the present he has been a graduate student in the Department of Physics at the University of Florida.

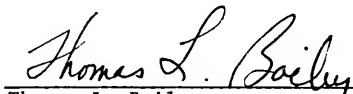Lawrence A. Woltz is married Carol Jean (Wideman) Woltz.

I certify that I have read this study and that in my opinion it conforms to acceptable standards of scholarly presentation and is fully adequate, in scope and quality, as a dissertation for the degree of Doctor of Philosophy.

Charles F. Hooper, Jr., Chairman
Professor of Physics

I certify that I have read this study and that in my opinion it conforms to acceptable standards of scholarly presentation and is fully adequate, in scope and quality, as a dissertation for the degree of Doctor of Philosophy.

James W. Dufty
Professor of Physics

I certify that I have read this study and that in my opinion it conforms to acceptable standards of scholarly presentation and is fully adequate, in scope and quality, as a dissertation for the degree of Doctor of Philosophy.

Thomas L. Bailey
Professor of Physics

I certify that I have read this study and that in my opinion it conforms to acceptable standards of scholarly presentation and is fully adequate, in scope and quality, as a dissertation for the degree of Doctor of Philosophy.

Billy S. Thomas
Associate Professor of Physics

I certify that I have read this study and that in my opinion it conforms to acceptable standards of scholarly presentation and is fully adequate, in scope and quality, as a dissertation for the degree of Doctor of Philosophy.

Kwan Y. Chen
Professor of Astronomy

This dissertation was submitted to the Graduate Faculty of the Department of Physics in the College of Liberal Arts and Sciences and to the Graduate Council, and was accepted as partial fulfillment of the requirements for the degree of Doctor of Philosophy.

August, 1982

_____

Dean for Graduate Studies
and Research